Kick matters: The impact of a new recoil model on the retention of hierarchical black-hole remnants in dense star clusters

Tousif Islam,[1,*] Digvijay Wadekar,[2,3] and Konstantinos Kritos[3]

[1]*Kavli Institute for Theoretical Physics, University of California Santa Barbara, Kohn Hall, Lagoon Rd, Santa Barbara, California 93106*
[2]*Weinberg Institute, University of Texas at Austin, Austin, Texas 78712, USA*
[3]*Department of Physics and Astronomy, Johns Hopkins University, 3400 N. Charles Street, Baltimore, Maryland, 21218, USA*

(Received 10 April 2026; accepted 22 July 2026; published 17 August 2026)

In a dense star cluster, hierarchical mergers are among the most promising pathways to forming massive black holes such as GW231123. A key factor determining whether a merger-remnant black hole will be retained in these environments and thus participate in subsequent hierarchical mergers is the recoil kick velocity. Analytic models for the recoil velocity are currently employed in nearly all population-synthesis frameworks. We instead use a state-of-the-art recoil-kick model gwModel_flow_prec [T. Islam and D. Wadekar, arXiv:2511.11536] developed from a combination of numerical-relativity and black-hole–perturbation-theory data, together with data-driven techniques such as normalizing flows and the post-Newtonian structure of the kick. Employing both back-of-the-envelope estimates and detailed N-body as well as semianalytical cluster simulations, we show that gwModel_flow_prec leads to a noticeable increase in the retention probability of hierarchical-merger remnants compared to the previously used analytic model and changes the mass and spin distribution of the black holes formed through hierarchical mergers. Additionally, we discuss the implications of our results in the context of massive binaries such as GW231123.

DOI: 10.1103/tchv-vdv5

I. INTRODUCTION

One of the consequences of binary black-hole (BBH) mergers in general relativity (GR) is the recoil kick imparted to the remnant black hole (BH) [1–3]. This kick arises from the rapid change in linear momentum during the merger and can reach velocities as large as $\sim$5000 km s^{-1} [2,4–11]. Over the past two decades, this phenomenon has been studied in detail using a combination of numerical relativity (NR) [1,12–35], black-hole perturbation theory (BHPT) [3,36–40], and post-Newtonian (PN) approximations [25,41–47], leading to a rich phenomenology. Building on these developments, several fast approximate models for the recoil velocity have emerged [13,22,23,29,30,34,36,37,47–54], and these are now routinely employed in gravitational-wave (GW) data analysis [55–58].

One of the key astrophysical implication of BBH mergers is the possibility of *hierarchical mergers* [59,60], in which BHs produced as merger remnants subsequently merge again. The initial, or first-generation (1G), BH population is expected to originate from stellar collapse and typically has masses $\lesssim 50 M_\odot$ [61,62]. However, when two 1G BHs merge, the resulting remnant, a second-generation (2G) BH, can exceed this mass scale. Subsequent mergers between 2G and 1G BHs, or between two 2G BHs, can then produce third-generation (3G) BHs. This process can of course continue further. This dynamical assembly mechanism is widely considered a promising pathway for forming intermediate-mass black-hole (IMBH) seeds and, ultimately, supermassive black holes [19,59,60,63–68]. Recently, several GW events, such as GW190521 [69] and GW231123 [70], have been interpreted as involving BHs with masses of order $100 M_\odot$ or higher. These observations have renewed interest in hierarchical-merger scenarios.

However, it is not guaranteed that all remnant BHs will participate in hierarchical mergers within clusters or galactic nuclei. A key ingredient in determining whether hierarchical mergers can occur is the interplay between the recoil kick velocity imparted to the remnant BH at merger and the escape velocity of the host dense star clusters [19,59,60,63–68]. If the kick velocity is significantly larger than the escape velocity, the remnant will be ejected from the host system (e.g., a globular cluster). Conversely, if the kick velocity is smaller than the escape velocity, the remnant BH will remain bound, albeit potentially displaced from the merger site. It can then return to

*Contact author: tousifislam@ucsb.edu

the center through efficient dynamical friction on a timescale that is smaller than the stellar relaxation time by a factor $\sim m_\star/m_{\rm BH}$, and the BH can subsequently participate in additional mergers.

In the past, hierarchical mergers have been studied extensively using back-of-the-envelope calculations applied to simplified cluster models, often incorporating varying assumptions about cluster astrophysics [19,59,60,63–68]. In parallel, significant effort has gone into modeling cluster dynamics, including hierarchical mergers [59,60,71,72], using N-body simulations [73,74], Monte Carlo methods [75], and semianalytical frameworks [76]. Various codebases such as Cluster Monte Carlo (CMC) [75,77], McFACTS [78], RAPSTER [76], FASTCLUSTER [79], cBHBd [80], and BPOP [81] have been developed to model the demographics of compact objects originating from dynamical channels. All these studies have almost invariably relied on analytic recoil-kick models [9,22,23,29,30], which were developed years ago from a relatively small NR dataset that was heavily biased toward equal-mass, aligned-spin binaries. We collectively refer to this model as the HLZ model (after the authors).

Islam and Wadekar [48] (hereafter IW25) recently presented an updated model gwModel_flow_prec[1] for the recoil kick based on a significantly larger dataset constructed from a combination of NR simulations and BHPT. Their model incorporates analytical insights from PN theory and leverages data-driven techniques such as normalizing flows to produce a more accurate recoil-velocity model than the analytic HLZ model. Furthermore, IW25 demonstrated that previously used analytic models tend to overestimate the kick in many regions of parameter space, which would artificially suppress the predicted retention efficiency of BHs undergoing hierarchical mergers. Previously, the predicted large recoil kicks disfavored hierarchical mergers as an efficient pathway for growing massive BHs in dense stellar clusters, motivating the community to instead explore alternative runaway formation channels—including successive tidal disruption events (e.g., Refs. [82,83]) and repeated stellar collisions (e.g., Ref. [84])—as viable mechanisms for producing massive BHs in this environment. The goal of our paper is to use our updated recoil kick model to reexamine hierarchical-merger pathways and quantify the resulting astrophysical implications.

To illustrate how the updated recoil-kick model can significantly affect several astrophysical conclusions from previous studies, we employ a range of dynamical population synthesis methods. First, we conduct a series of semianalytical simulations that vary initial mass and spin distributions, as well as the binary pairing functions, to explore how many BHs can form and how massive they can become through hierarchical mergers under different recoil-kick prescriptions. Next, we perform approximately 7500 detailed astrophysical cluster simulations using the semianalytical cluster evolution code RAPSTER. By adopting a representative set of cluster properties and varying random seeds, we highlight how the landscape of hierarchical mergers is altered when using the new recoil model compared to older prescriptions.

The remainder of this paper is organized as follows. In Sec. II, we outline our approach to modeling the recoil kick. Section III presents a series of simplified numerical experiments using our baseline model, aimed at elucidating the effects of model uncertainties, the initial BH population, and binary pairing functions on the resulting masses and spins of BHs formed through hierarchical mergers. These studies make use of the gwGenealogy package,[2] which we have developed as part of this work to offer a straightforward, unified, and publicly accessible framework for studying hierarchical mergers.

Building upon the insights from these simplified calculations, we next move to more detailed and realistic cluster simulations in Sec. IV, exploring various recoil-kick prescriptions. These simulations use the RAPSTER package[3] [85] and CMC [77]. Throughout Secs. III and IV, we relate our findings to the population of massive BHs associated with the GW231123 event. In Sec. V, we discuss the broader implications of our results and outline potential directions for future work.

II. MODEL FOR THE RECOIL VELOCITY

A BBH merger is characterized by two BHs with masses $m_{1,2}$ (with $m_1 \geq m_2$), dimensionless spin magnitudes $\chi_{1,2} \in [0,1]$, and four spin-orientation angles $\{\theta_1, \theta_2, \phi_1, \phi_2\}$. The angles $\{\theta_1, \theta_2\} \in [0, \pi]$ denote the tilt of each spin vector relative to the orbital angular-momentum axis, while $\{\phi_1, \phi_2\} \in [0, 2\pi]$ specify the in-plane spin angles projected onto the orbital plane. The mass ratio is denoted by $q \coloneqq \frac{m_1}{m_2} \geq 1$. The remnant BH has mass m_f and dimensionless spin χ_f, and the magnitude of the recoil (kick) velocity is denoted by v_f. In this work, we focus exclusively on the magnitude of the kick, as the kick direction is not especially relevant for hierarchical mergers in clusters that have isotropic symmetry.

To compute recoil kick velocities, essentially all N-body cluster-simulation codes and semianalytical frameworks rely on the semianalytical HLZ model [9,22,23,29,30]. More recently, some theoretical studies [60,86] have employed NR surrogate models, which offer improved accuracy relative to HLZ. However, these surrogate models are restricted to mass ratios $1 \leq q \leq 4$ for precessing systems and $1 \leq q \leq 8$ for aligned-spin systems, and they are approximately 3 orders of magnitude slower than the semianalytical HLZ fits, limiting their applicability in large-scale cluster simulations. To overcome these challenges,

[1] https://github.com/tousifislam/gwModels.

[2] https://github.com/tousifislam/gwGenealogy.

[3] https://github.com/Kkritos/Rapster.

IW25 have recently developed gwModel_flow_prec, a normalizing-flow-based model that accurately captures the distribution of recoil kick velocities arising from varying spin orientations.

To explicitly quantify the differences between the new recoil model gwModel_flow_prec and the earlier prescription HLZ, we compute recoil kick velocity distributions for 1000 randomly selected combinations of the mass ratio $q \in [1, 20]$ and spin magnitudes $|\chi_{1,2}| \in [0, 1]$. For each combination of mass ratio and spin magnitudes, we draw 5000 spin orientation angles from an isotropic distribution, i.e., $\cos\theta_{1,2} \in \mathcal{U}(-1, 1)$ and $\phi_{1,2} \in \mathcal{U}(0, 2\pi)$.

To measure the discrepancy between the kick velocity distributions predicted by the two models, we compute the Jensen-Shannon divergence (JSD). The JSD between two probability distributions p_1 and p_2 is defined as [87]

$$\mathrm{JSD}(p_1||p_2) = \frac{1}{2}\mathrm{KL}(p_1||m) + \frac{1}{2}\mathrm{KL}(p_2||m), \quad (1)$$

where $m = \frac{1}{2}(p_1 + p_2)$ is their pointwise mean and KL denotes the Kullback-Leibler divergence [87]

$$\mathrm{KL}(X||Y) = \int X(x)\log\left(\frac{X(x)}{Y(x)}\right)dx. \quad (2)$$

The JSD is symmetric and bounded, $0 \leq \mathrm{JSD}(p_1||p_2) \leq \log 2 \approx 0.693$. Values $\mathrm{JSD} \lesssim 0.02$ indicate virtually indistinguishable distributions, while $\mathrm{JSD} \gtrsim 0.1$ signifies substantial differences; intermediate values correspond to moderately distinct distributions.

In Fig. 1, we show the JSD as a function of the binary parameter space. We find that the kick velocity distributions predicted by gwModel_flow_prec and HLZ differ significantly across large regions of parameter space. In particular, when one or both spin magnitudes are small, the JSD increases markedly, indicating substantial discrepancies between the two models. In contrast, the two prescriptions yield more similar kick distributions for nearly equal-mass binaries except for slowly spinning binaries. As the mass ratio becomes increasingly asymmetric, the differences between the models grow. Note that separate versions of Fig. 1 for the low and high mass ratio cases were presented in IW25 (see their Figs. 7 and 8). They also show that gwModel_flow_prec agrees much better with NR surrogate models compared to HLZ for the low mass ratio case (which is the regime where the NR surrogate model is expected to be more accurate compared to HLZ).

III. BACK-OF-THE-ENVELOPE CALCULATIONS

We use gwGenealogy to perform a series of experiments to build intuition about hierarchical mergers under simplified astrophysical assumptions. Each experiment is carried out twice: once using the HLZ recoil model and once using the gwModel_flow_prec recoil model.

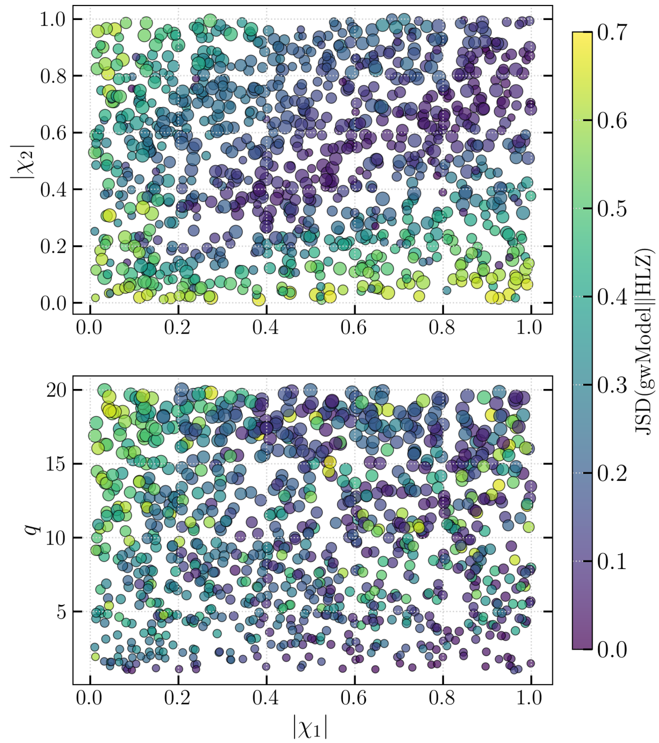

FIG. 1. We show the Jensen-Shannon divergence (color-coded) between the kick-velocity distributions predicted by the new gwModel_flow_prec model and the widely-used analytic model HLZ. The kick distributions for each point in the $q, |\chi_1|, |\chi_2|$ space are generated by drawing 5000 spin orientation angles from an isotropic distribution. The symbol size scales with the mass ratio: smaller circles correspond to smaller q, while larger circles correspond to larger q. There are substantial discrepancies between the two models when one or both spin magnitudes are small and/or when the mass ratio becomes increasingly asymmetric. More details are in Sec. II.

For the initial mass function (IMF) of the 1G BHs, following Refs. [59,65,88,89], we consider several distributions: (i) a uniform distribution for $m_{\mathrm{BH}} \in [3, 60]M_\odot$ (unless otherwise specified) and (ii) a power-law distribution $p(m) \propto m^\alpha$ (with $\alpha = -2.4$) restricted to the same mass range. For the 1G BHs, we generally do not consider masses beyond $60M_\odot$ because pair instability and pulsational pair instability in massive helium cores are expected to suppress the formation of 1G BHs in this mass range [90], although the exact value of the upper limit is not known and depends on the details of nuclear burning physics [91].

For the initial spin distribution of 1G BHs, we explore two classes of populations: a *high-spin* population, where the spin magnitudes are drawn uniformly as $\chi_{1,2} \in [0, 1]$, and a *low-spin* population (following Ref. [92]), where $\chi_{1,2} \in [0, 0.1]$. In addition, we consider Beta distributions (following Ref. [93]) over the same range of spin magnitudes. Unless otherwise specified, spin-orientation angles are sampled isotropically and motivated by the spherical symmetry of potential host environments such as dense star cluster.

We also investigate several binary pairing functions that determine how the component masses $m_{1,2}$ are selected. First, we consider *random pairing*, in which m_1 and m_2 are drawn independently from the underlying 1G mass distribution. We then examine two forms of *selective pairing*, in which m_1 is drawn from the IMF but the distribution of m_2 is conditioned on m_1. Following Refs. [59,65,85,88,89], we consider models of the form

$$p(m_2|m_1) = m_2^{\beta} \quad (\text{model A}) \tag{3}$$

with $\beta = 6.7$, and models of the form

$$p(m_2|m_1) = (m_1 + m_2)^{\gamma} \quad (\text{model B}) \tag{4}$$

with $\gamma = 4$.

A. Comparison of retention probabilities

First, we investigate how the retention probability changes when using gwModel_flow_prec in place of the older HLZ model.

In Fig. 2, we show the probability (estimated over 10^4 Monte Carlo realizations to ensure that the results have converged) of retaining the remnant of a BBH merger as a function of the mass ratio q and the maximum spin magnitude $\chi_{\rm max}$, for several cluster escape velocities $v_{\rm esc} = 25$, 50, 100, 150, 200, and 500 km s^{-1}, using both the gwModel_flow_prec and HLZ prescriptions. We do not vary the individual BH masses here because the recoil kick depends only on the mass ratio and spins, not on the absolute masses. For each q, we draw the spin magnitudes $\chi_{1,2}$ uniformly from $[0, \chi_{\rm max}]$, and we sample spin-orientation angles isotropically. The resulting retention probability is shown as a color map.

For $v_{\rm esc} = 50$ km s^{-1}, we find that almost no remnants are retained when kicks are computed with HLZ. However, when using gwModel_flow_prec, the retention probability increases significantly for higher mass ratios ($q \gtrsim 6$) and for near-equal-mass binaries with $\chi_{\rm max} \lesssim 0.6$. Similar trends appear for escape velocities of 100 and 150 km s^{-1}. For example, at $v_{\rm esc} = 100$ km s^{-1}, the retention probability increases from nearly zero to values in the range 0.2–0.4 for mass ratios between $q \approx 1.5$ and $q \approx 7$ when switching from HLZ to gwModel_flow_prec. For $v_{\rm esc} = 500$ km s^{-1}, the escape velocity is sufficiently large that nearly all remnant BHs are retained regardless of whether HLZ or gwModel_flow_prec is used, and the differences between the two models largely vanish.

To quantify the differences in retention probabilities predicted by the two models, we compute the JSD between the retention-probability distributions (over all mass ratio and maximum spin values) obtained from gwModel_flow_prec and HLZ at several escape velocities. We find JSD values of 0.351, 0.467, 0.098, 0.100, 0.051, and 0.021 for escape velocities $v_{\rm esc}$ of 25, 50, 100, 150, 200, and 500 km s^{-1}, respectively. This reaffirms that the retention probabilities are quite different between gwModel_flow_prec and HLZ for escape velocities less than 500 km s^{-1}. We repeat the same experiment using initial spin magnitudes drawn from a Beta distribution over $[0, \chi_{\rm max}]$. We find qualitatively similar differences between the two models (not shown).

B. Probability of forming an intermediate-mass black hole

Next, following Ref. [89], we perform another simplified simulation with minimal assumptions to assess whether hierarchical mergers can lead to the formation of IMBHs with a mass of $100 M_\odot$ or beyond. In addition, we also ask whether the BH mass can reach $150 M_\odot$ (remnant mass of GW190521) and $250 M_\odot$ (remnant mass of GW231123).

We begin by choosing a metallicity Z for the host cluster, which sets the maximum mass of BHs that can form through stellar collapse. For the stellar population, we consider zero-age main-sequence (ZAMS) masses in the range $[0.08, 150] M_\odot$. We then sample 5000 stellar masses from a Kroupa mass function. To compute the mass of the corresponding 1G BHs, we use the updated single-star evolution (SSE) delayed prescription of Refs. [94–96], as implemented in Ref. [85]. This framework incorporates the effects of pulsational pair-instability supernovae and pair-instability supernovae, thereby producing the expected upper mass gap in the stellar-origin BH population [97].

In Fig. 3, we show the resulting remnant BH masses as a function of the progenitor ZAMS mass and the metallicity. Typically, at low metallicities (for example, $Z = 0.0002$), stellar collapse can produce more massive BHs, with masses reaching up to $\sim 45 M_\odot$. As the metallicity increases toward solar values, the maximum BH mass attainable through stellar collapse decreases, with typical upper limits of only $\sim 15 M_\odot$ in our prescription. Note that this upper limit may vary depending on the specific prescription adopted [61,90,91,94,95].

On the other hand, collisions or mergers of massive stars may produce BH remnants in the high-mass gap, i.e., beyond $60 M_\odot$. Motivated by this possibility, we consider an additional population of BHs with masses in the range $[10, 100] M_\odot$ [98–100]. Following Ref. [89], we treat BHs in this mass range as *seed* BHs. As in the previous section, we draw spin magnitudes for both the 1G BHs and seed BHs from $[0, \chi_{\rm max}]$. Additionally, we sample spin-orientation angles isotropically for all binaries and assume a mass-weighted pairing function $\propto (m_1 + m_2)^4$. These seed BHs are allowed to merge with the 1G BH population, and any remnant BH that is not ejected from the host environment is permitted to participate in subsequent hierarchical mergers. The masses and spins of the BBH merger remnants are computed using semianalytical fitting formulas calibrated

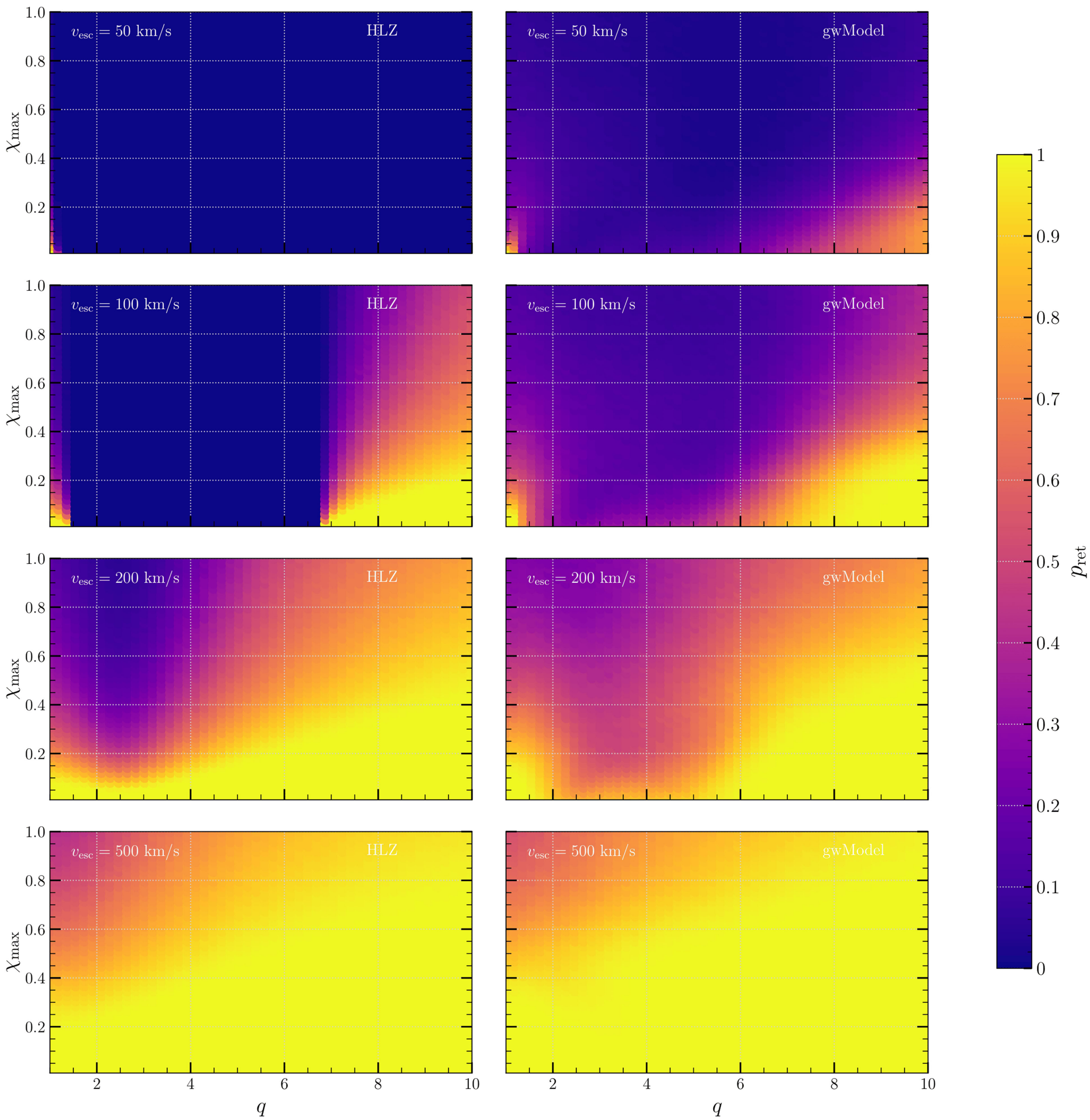

FIG. 2. Probability of retaining the merger remnant of a BBH (shown by the color bar) as a function of the BBH mass ratio and the maximum BH spins, shown for different cluster escape speeds: 50–500 km s^{-1} (increasing from top to bottom). The left columns show the results obtained using the HLZ recoil-kick model, while the right columns show the results for the gwModel_flow_prec. The BH spins are drawn from a uniform distribution in the range $[0, \chi_{max}]$, and spin angles are chosen isotropically. Details are in Sec. III A.

to NR data [101,102]. These fits are known to be highly accurate, with typical modeling errors below 1%, and can therefore be treated as sufficiently precise for astrophysical applications. For the recoil kick, we again consider both the gwModel_flow_prec and HLZ prescriptions. We then compute the fraction of seed BHs that eventually produce an IMBH of at least $100 M_\odot$ or $250 M_\odot$. We denote this IMBH-formation probability by p_{IMBH}. In this experiment, we do not allow the seeds to merge among themselves, nor do we permit the 1G BHs to merge with one another. All mergers occur exclusively between a 1G BH and a seed (or its remnant).

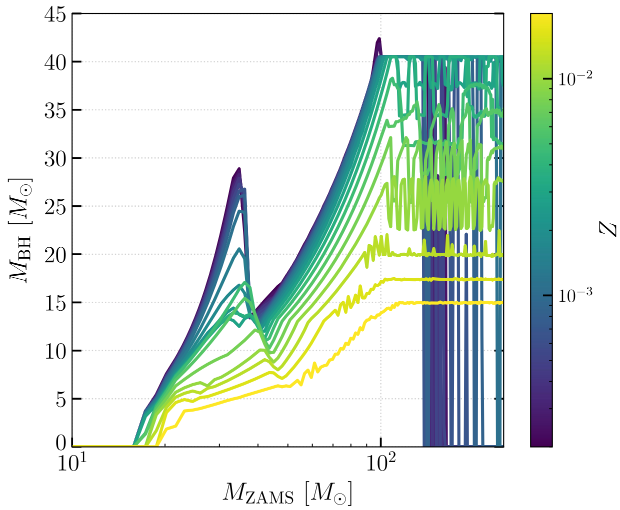

FIG. 3. For creating compact objects in our cluster simulations, we use the updated single-star evolution delayed prescription of Refs. [94–96]. Here, we show the masses of remnant BHs formed from stellar collapse as a function of the progenitor star's ZAMS mass, with metallicity indicated in the color bar. More details are in Sec. III B.

To explore the dependence on the host-cluster potential, we consider a range of escape velocities, $v_{\rm esc} \in [50, 500]$ km s^{-1}, and calculate the IMBH-formation probability, $p_{\rm IMBH}$. To quantitatively assess how the two recoil-kick prescriptions differ in their predicted IMBH-formation probabilities, we further compute the differences in probabilities

$$\Delta p_{\rm IMBH} = p_{\rm IMBH}^{\rm gwModel}(M_{\rm seed}^{\rm BH}, \chi_{\rm max}) - p_{\rm IMBH}^{\rm HLZ}(M_{\rm seed}^{\rm BH}, \chi_{\rm max}). \quad (5)$$

A positive value of $\Delta p_{\rm IMBH}$ indicates that gwModel_flow_prec predicts a higher overall probability of IMBH formation. Our results are shown in Fig. 4. For metallicity $Z = 0.005$, we find that for $v_{\rm esc} \lesssim 100$ km s^{-1} the probability of forming an IMBH of mass $250M_\odot$ is extremely small across all seed masses, since most mergers produce recoil velocities of order 50–100 km s^{-1}, leading to the ejection of the merger remnants. We therefore omit these cases from the figure. For an escape velocity of $v_{\rm esc} = 200$ km s^{-1}, only a small fraction of seed BHs grow to IMBH masses. The difference between the two recoil prescriptions is correspondingly small, with an average probability difference of $\langle \Delta p_{\rm IMBH} \rangle = 0.0018 \pm 0.0152$. In contrast, for $v_{\rm esc} = 500$ km s^{-1}, the IMBH-formation probability becomes substantially larger and gwModel_flow_prec systematically predicts higher formation probabilities than HLZ, with an average probability difference of $\langle \Delta p_{\rm IMBH} \rangle = 0.0737 \pm 0.0361$. In particular, many seed BHs with masses of ∼$60M_\odot$–$90M_\odot$ are able to grow to masses exceeding $250M_\odot$. In most realizations, the maximum IMBH mass produced in this simplified setup is approximately $280M_\odot$.

For an escape velocity of 50 km s^{-1}, gwModel_flow_prec predicts a higher probability of forming a $100M_\odot$ IMBH in 1% of the parameter space compared to HLZ. The corresponding fractions are 20.8%, 31.7%, and 100% for escape

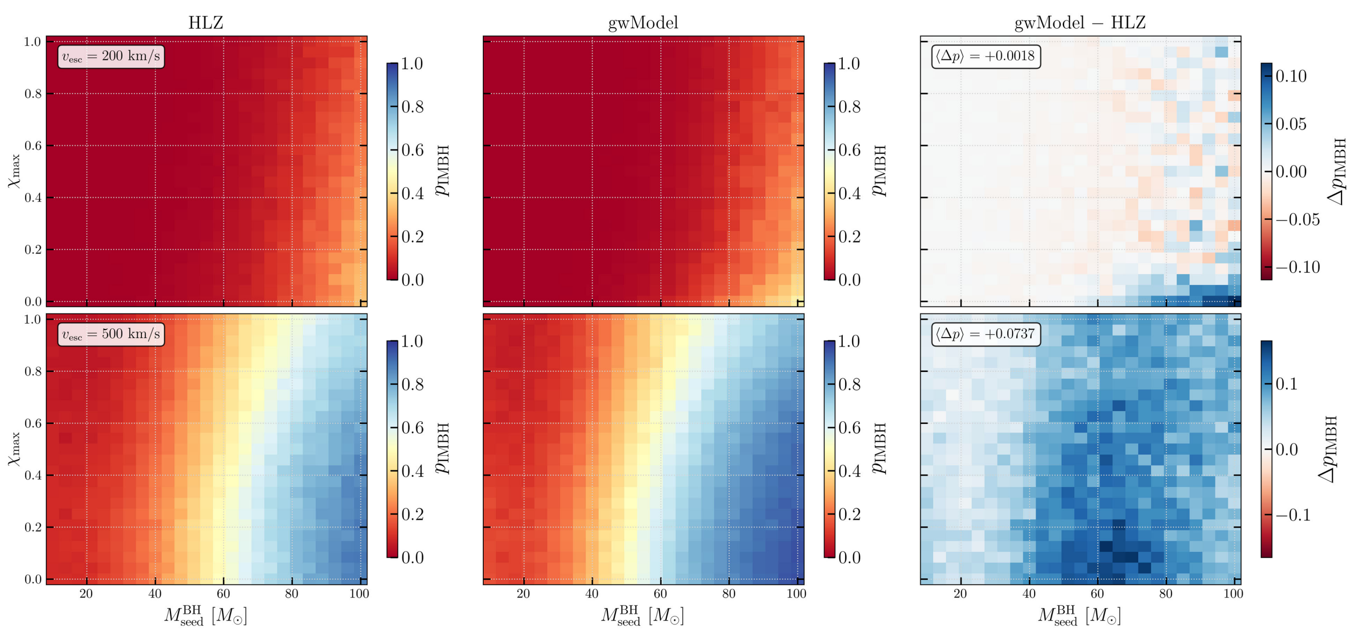

FIG. 4. Probability of forming a BH with mass at least $250M_\odot$ through successive mergers as a function of the seed-BH mass and the maximum spin magnitude, shown for escape velocities of 200 km s^{-1} (top panels) and 500 km s^{-1} (bottom panels). The left and middle columns show the IMBH-formation probability predicted by the HLZ and gwModel_flow_prec recoil-kick prescriptions, respectively. The right column shows the difference between the two models, $\Delta p_{\rm IMBH} = p_{\rm IMBH}^{\rm gwModel} - p_{\rm IMBH}^{\rm HLZ}$. For each escape velocity, we also report the mean difference $\langle \Delta p \rangle$. The BH spin magnitudes are drawn uniformly from the range $[0, \chi_{\rm max}]$, and we adopt a metallicity of $Z = 0.005$. Details are in Sec. III B.

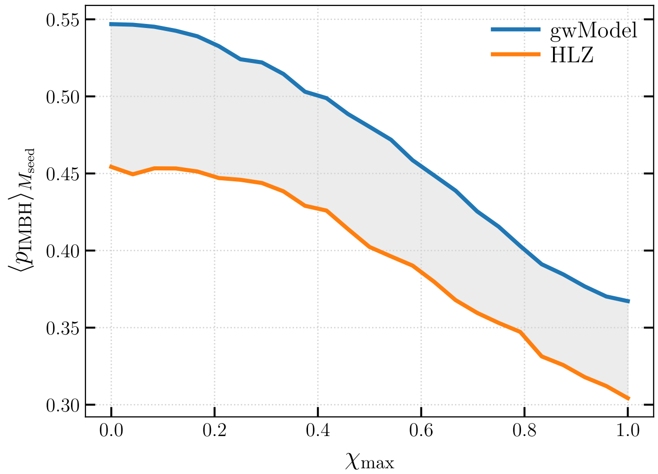

FIG. 5. Probability of forming an IMBH with mass at least $250 M_\odot$, averaged over the seed-BH mass distribution, as a function of the maximum spin magnitude $\chi_{\rm max}$ for an escape velocity of $v_{\rm esc} = 500\ {\rm km\,s^{-1}}$ and metallicity $Z = 0.005$. The blue and orange curves show the predictions of the gwModel_flow_prec and HLZ recoil-kick prescriptions, respectively. Details are in Sec. III B.

velocities of 150, 200, and 500 $\rm km\,s^{-1}$, respectively. This qualitative behavior remains the same when comparing the probabilities of forming IMBHs with masses of $150 M_\odot$ and $250 M_\odot$. We find that these results are not strongly dependent on the assumed maximum mass of the seed BHs (not shown).

To further quantify the differences between the recoil prescriptions in an interpretable manner, Fig. 5 shows the IMBH-formation probability averaged over the seed-BH mass distribution, $\langle p_{\rm IMBH}\rangle_{M_{\rm seed}}$, as a function of the maximum spin magnitude, $\chi_{\rm max}$, for $Z = 0.005$, $v_{\rm esc} = 500\,{\rm km\,s^{-1}}$, and an IMBH mass threshold of $250 M_\odot$. Across the entire range of $\chi_{\rm max}$, gwModel_flow_prec predicts a systematically higher IMBH-formation probability than HLZ, reflecting the larger retention fraction of merger remnants. The difference between the two models is most pronounced for low spin magnitudes and gradually decreases as $\chi_{\rm max}$ increases, although gwModel_flow_prec remains more efficient at producing IMBHs throughout the parameter space considered here. Similar trends are obtained for other escape velocities and metallicities (not shown).

C. Comparison of the mass and spin distributions across merger generations

Our next set of experiments tracks the masses and spins of retained BHs across successive merger generations in simplified cluster environments. In hierarchical merger scenarios, we define the BH generation as follows. BHs formed through direct stellar collapse are denoted as 1G. BHs formed via the merger of two 1G BHs are classified as second generation. BHs formed through the merger of a 2G BH with either a 1G or another 2G BH are classified as third generation, and so on.

We use the same prescriptions as in Sec. III B to compute the masses and spins of the remnant BHs after each BBH merger. For the recoil kick, we consider both the gwModel_flow_prec and HLZ prescriptions. We begin with a population of 5000 1G BHs. Unless otherwise specified, the BH masses are drawn either from a uniform distribution or from a power-law distribution over the range $[3, 60] M_\odot$ (see Sec. III). Similarly, the 1G BH spin magnitudes are drawn either from a uniform distribution or from a Beta distribution over the range [0, 1] (high-spin case) or [0, 0.1] (low-spin case). We consider both random and selective pairing prescriptions (see Sec. III) when assembling BBH systems. To mimic the diversity of cluster environments, we assign escape velocities drawn from the range $[1, 300]\ {\rm km\,s^{-1}}$, using either a uniform or a Gaussian distribution. This range spans the escape velocities expected in a broad class of dense stellar systems. Alternatively, when modeling an individual cluster, the escape velocity can be fixed to a specified value.

Each binary is merged to produce a population of 2G BHs. For every merger remnant, we compare the recoil kick velocity to the assigned escape velocity and determine whether the remnant is retained. Retained 2G BHs are subsequently allowed to merge among themselves and with 1G BHs, producing a population of 3G BHs. This procedure is repeated iteratively, and we track the growth of BHs up to the fifth merger generation. We perform these experiments for a variety of initial mass distributions, spin distributions, pairing prescriptions, and escape-velocity distributions. In Table I, we summarize the assumptions

TABLE I. Summary of the hierarchical-merger experiments presented in Sec. III C. We vary one physical ingredient at a time (except for case 6) relative to the baseline model (case 1). Here, IMF denotes the initial BH mass distribution, and ISF denotes the initial BH spin distribution.

Label	Case	IMF	ISF	Pairing	$v_{\rm esc}$
Default	1	Uniform	Uniform	Random	Uniform
Power law	2	Power law	Uniform	Random	Uniform
Model A	3	Uniform	Uniform	Model A	Uniform
Model B	4	Uniform	Uniform	Model B	Uniform
Low spin	5	Uniform	Uniform ([0, 0.1])	Random	Uniform
Beta	6	Uniform	Beta	Model B	Gaussian

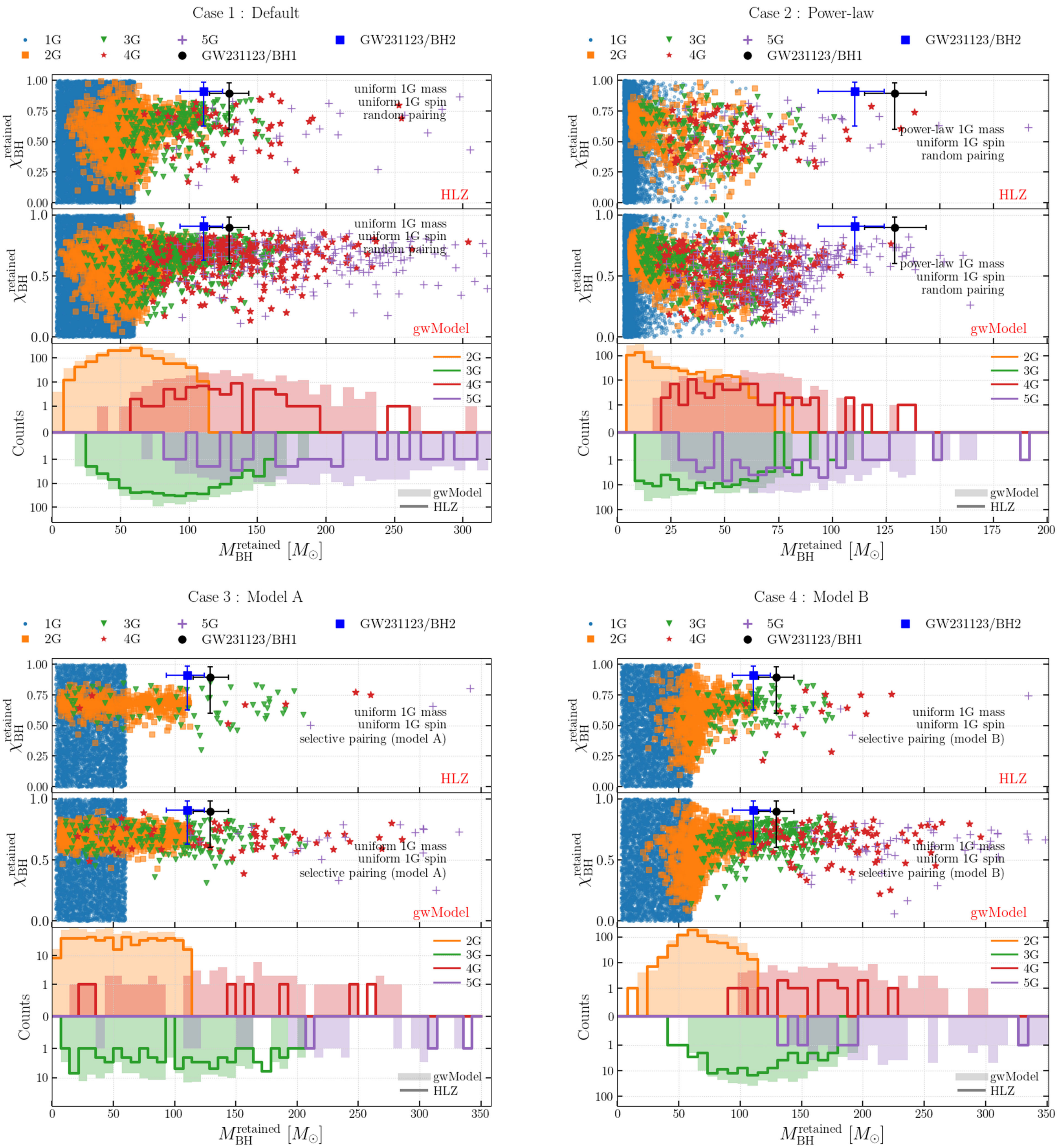

FIG. 6. Distribution of retained BH masses and spins across five merger generations. For reference, we show the mass and spin inference of BHs in the GW231123 binary in black and blue error bars throughout the paper. In each panel, the upper subplot corresponds to the HLZ model, and the middle subplot corresponds to the gwModel_flow_prec, whereas the lower subplot shows the mass distribution of the retained remnants. The spins of the 1G BH population are drawn uniformly from [0, 1], and the initial BH masses are drawn from $[3, 60]M_\odot$. We vary the initial mass distribution (uniform/power law) and the pairing function [random/model A/model B; see Eqs. (3) and (4)] one at a time: uniform IMF with random pairing (upper left), power-law IMF with random pairing (upper right), uniform IMF with model A pairing (lower left), and uniform IMF with model B pairing (lower right). In all cases, escape velocities are drawn uniformly from [1, 300] $\mathrm{km\,s^{-1}}$, typical of dense stellar clusters. Setups for these hierarchical-merger experiments are summarized in Table I. Details are in Sec. III C.

adopted in the different hierarchical-merger experiments considered in this section.

In Fig. 6, we show the distributions of retained BH masses and spins across five merger generations. In each panel, the upper subplot corresponds to the `HLZ` recoil-kick prescription, the middle subplot corresponds to gwModel_flow_prec, and the lower subplot shows the distribution of retained BH masses for each merger generation. For reference, we also show the inferred masses and dimensionless spins of the two BHs in GW231123. The primary BH has $m_1 = 129.1^{+14.7}_{-14.0} M_\odot$ and $\chi_1 = 0.89^{+0.09}_{-0.29}$, while the secondary BH has $m_2 = 110.6^{+13.7}_{-17.2} M_\odot$ and $\chi_2 = 0.91^{+0.08}_{-0.28}$, where the uncertainties denote the 90% credible intervals. Our main findings from Fig. 6 are as follows: (1) The distributions of BH masses and spins across successive generations change noticeably when replacing the `HLZ` kick prescription with the more accurate gwModel_flow_prec, regardless of the assumed initial mass or pairing function. (2) The gwModel_flow_prec consistently predicts a larger number of BHs occupying the mass-spin region consistent with the inferred properties of GW231123. (3) We find that pairing model A generally produces fewer massive BHs across successive merger generations, whereas the pairing model B yields a noticeably larger population of high-mass BHs. (4) Finally, when the 1G BH population is drawn from a uniform mass distribution instead of a power-law distribution, we find that more massive BHs are produced through hierarchical mergers.

Next, we show the impact of the initial spin distribution in Fig. 7. The top panel shows results for 1G BH spins drawn uniformly in a narrow range [0, 0.1], while assuming a uniform initial mass function and random pairing. We find that slowly spinning initial BHs produce more massive merger remnants than an initial spin distribution in [0, 1] (cf. Fig. 6, upper left). The bottom panel of Fig. 7 shows the impact of varying several ingredients simultaneously. We show the distributions of retained BH masses and spins across five merger generations for a setup in which the initial BH spin magnitudes are drawn from a Beta distribution over [0, 1]; the initial BH masses are drawn uniformly from $[3, 60] M_\odot$; and a selective, mass-weighted pairing function is used when forming binaries. In addition, escape velocities are sampled from a Gaussian distribution spanning $[1, 300]\ \mathrm{km\,s^{-1}}$.

To better quantify the impact of the recoil prescription across the different hierarchical-merger experiments, in Fig. 8, we show the percentage differences between the gwModel_flow_prec and `HLZ` predictions for three quantities: the number of retained BHs, the median retained BH mass, and the median retained BH spin. Positive values indicate that the corresponding quantity is larger when using gwModel_flow_prec. For each of the six cases summarized in Table I, we perform 10 independent realizations with 25,000 initial BHs and report the mean and standard

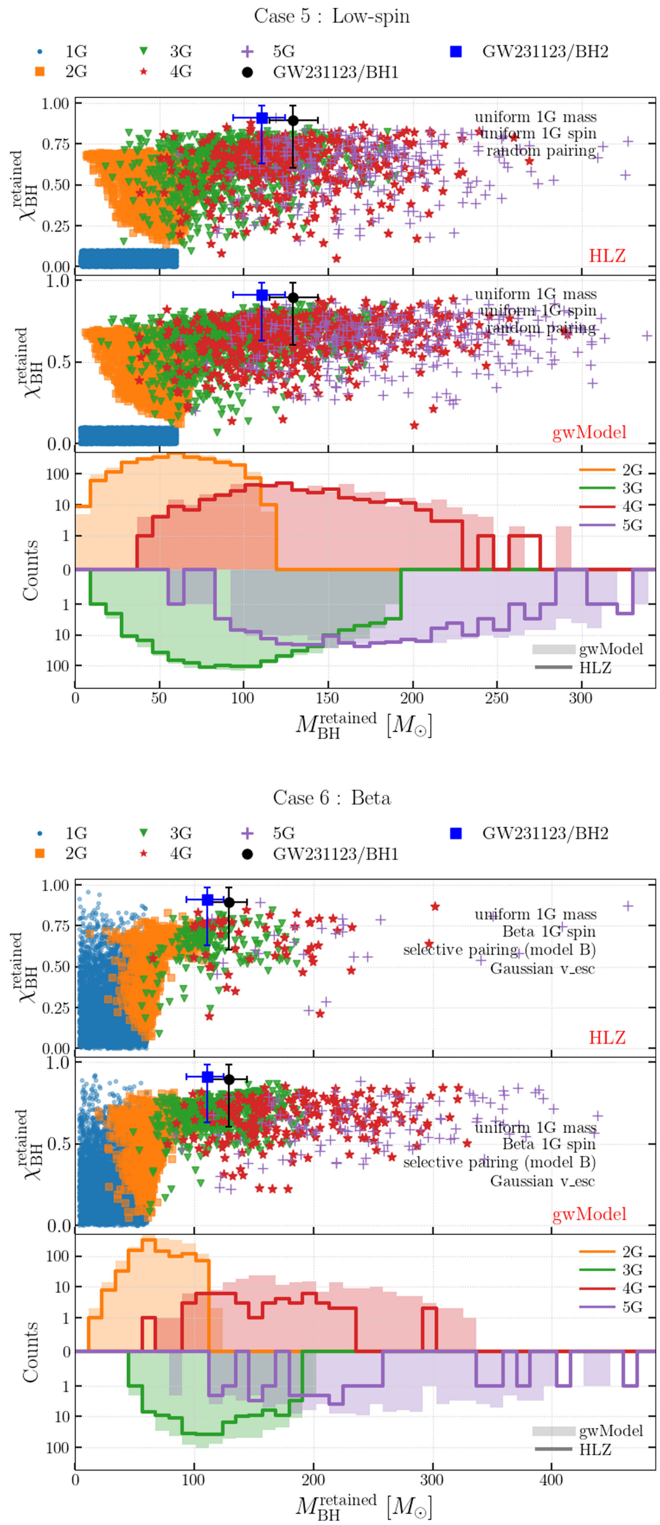

FIG. 7. Same as the top-left panel of Fig. 6 but exploring different distributions of 1G BH spins. Top: 1G BH spins drawn uniformly from [0, 0.1] instead of [0, 1]. Bottom: 1G BH spins are drawn from the range [0, 1] following a Beta distribution. Setups for these hierarchical-merger experiments are summarized in Table I. Additionally, we use the mass-weighted pairing from Eq. (4) when forming binaries, and a Gaussian distribution for escape velocities instead of a uniform distribution. Details are in Sec. III C.

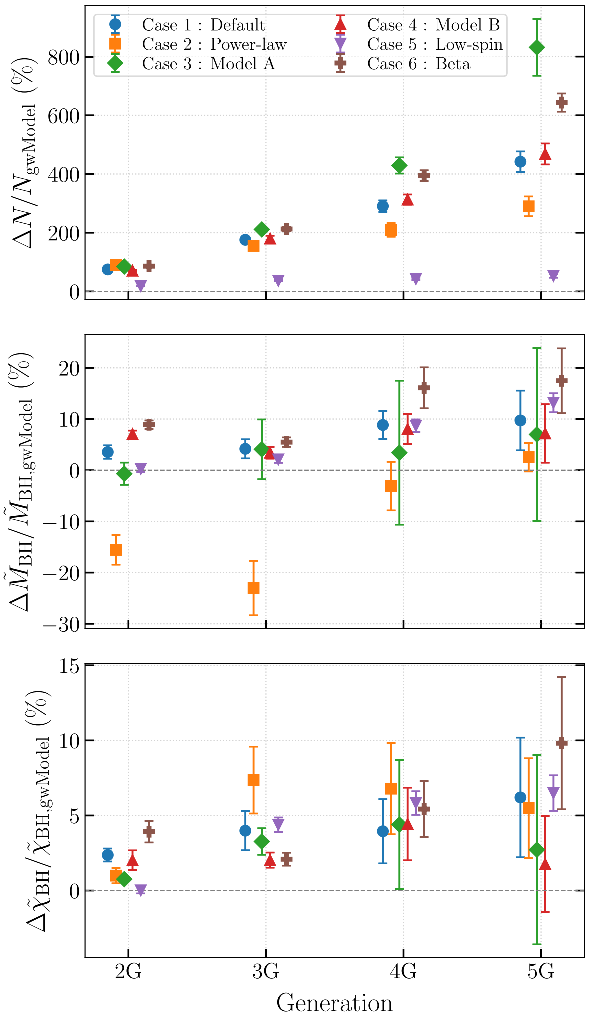

FIG. 8. Percentage differences between the predictions of gwModel_flow_prec and HLZ for the number of retained BHs (ΔN), the median retained BH mass ($\Delta\tilde{M}_{\rm BH}$), and the median retained BH spin ($\Delta\tilde{\chi}_{\rm BH}$) as a function of merger generation. Positive values indicate that the corresponding quantity is larger for gwModel_flow_prec. Results are shown for the six hierarchical-merger experiments summarized in Table I. Each point represents the average over 10 realizations with 25000 initial BHs, while the error bars denote the standard deviation among realizations. Details are in Sec. III C.

deviation across the realizations. The most striking effect is observed in the number of retained BHs. Across all six cases, gwModel_flow_prec predicts systematically larger retained populations than HLZ, with the relative difference increasing with merger generation. Depending on the adopted assumptions, the number of retained 5G BHs can exceed the HLZ prediction by several hundred percent. In contrast, the median masses and spins of the retained BHs are affected at a more modest level. We find that gwModel_flow_prec generally produces BHs that are a few to $\sim$10% more massive and have spins that are typically a few percent larger than those obtained with HLZ. These results indicate that the primary effect of the updated recoil prescription is to enhance remnant retention, while producing more moderate changes in the masses and spins of the retained BH population.

We have also experimented with other combinations (not shown) of initial mass functions (such as power law) and pairing functions (such as model A and model B). As in previous cases, we find that the gwModel_flow_prec prescription produces more massive BHs than the HLZ model.

D. Comparison of the retention probability across cluster properties

Our next experiment incorporates more realistic astrophysical information about globular-cluster properties into the model. We generate 1500 cluster realizations and simulate 5000 BBH mergers in each realization. The cluster metallicity is drawn uniformly in logarithmic space between 0.0002 and 0.02, the cluster mass between 10^4 and $10^7 M_\odot$, and the half-mass radius between 0.1 and 10 pc. We emphasize that this calculation is not intended to represent a population-weighted cluster ensemble. Rather, its purpose is to explore how remnant retention depends on cluster properties and to identify the regions where the gwModel_flow_prec and HLZ recoil prescriptions differ most strongly.

For the 1G BHs, the spin magnitudes $\chi_{1,2}$ are drawn uniformly from [0, 1], and all 1G BHs are assumed to form via stellar collapse. The ZAMS masses of the progenitor stars, $M_{\rm ZAMS}$, are sampled uniformly from the range $[10, 150]M_\odot$. The cluster metallicity determines the resulting distribution of 1G BH masses. The cluster mass and half-mass radius determine the (virialized) cluster escape velocity, $v_{\rm esc}$ [85]:

$$v_{\rm esc} \simeq 26\ {\rm km\,s^{-1}} \left(\frac{M_{\rm cl}}{10^5 M_\odot}\right)^{1/2} \left(\frac{r_h}{1\ {\rm pc}}\right)^{-1/2}. \tag{6}$$

As in previous sections, spin-orientation angles are drawn isotropically. We assume random mass pairing between the two BHs forming a binary. We then compute the retention probability of the 1G + 1G merger remnants.

In Fig. 9, we show the retention probability as a function of cluster mass ($M_{\rm cl}$ and half-mass radius $r_{\rm h}$). We observe lines of nearly constant escape velocity that govern the retention probability. As expected, more massive clusters with smaller half-mass radii tend to retain a larger fraction of 1G + 1G merger remnants. Furthermore, when using gwModel_flow_prec, a larger fraction of remnants are retained compared to the HLZ prescription, consistent with the fact that HLZ generally predicts higher kick velocities. In particular, for clusters with escape velocities in the range 20 to 200 $\rm km\,s^{-1}$, the differences in retention probabilities predicted by gwModel_flow_prec and HLZ become more pronounced. Additionally, we find that cluster metallicity has little effect on the retention probability (not shown in

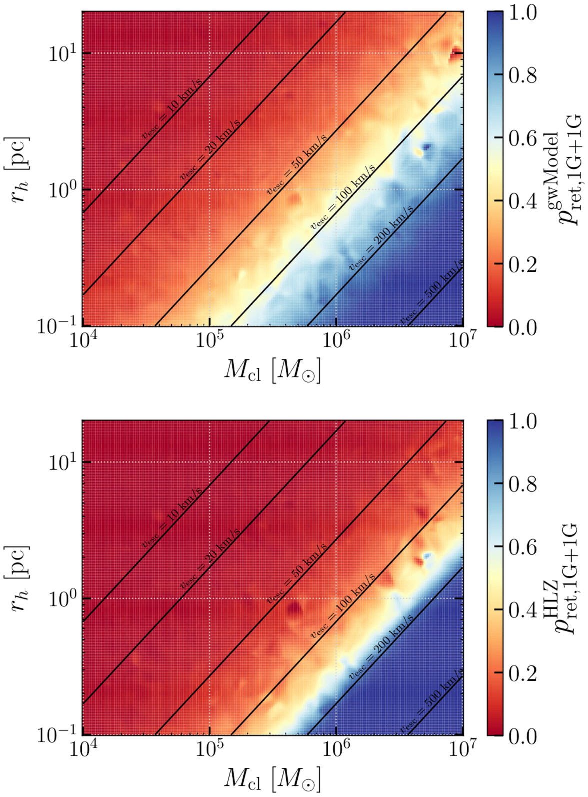

FIG. 9. In Figs. 6 and 7, we had marginalized over cluster properties (using the prior for cluster escape velocities as uniform over $[1, 300]$ km s^{-1}). Here, we show the variation of the probability of retaining the merger remnant of two 1G BHs with cluster mass and half-mass radius (for reference, the lines of constant escape velocity are in black). The top (bottom) panel shows results obtained using the gwModel_flow_prec (HLZ) recoil-kick prescription. The largest differences in the kick models are observed in clusters with v_{esc} in the range 20–200 km s^{-1}. Other population properties for BH mass and spin distributions are similar to the top-right panel of Fig. 6. Details are in Sec. III D.

the figure). This is not unexpected; although metallicity influences the masses of the 1G BHs, the recoil kick depends primarily on the mass ratio. Under random pairing, the mass-ratio distribution is only weakly sensitive to the underlying BH mass distribution, leading to similar retention probabilities across metallicities.

IV. DETAILED CLUSTER SIMULATIONS

We now move to more detailed cluster-evolution simulations that self-consistently follow the collisional dynamics, stellar and binary evolution, dynamical interactions, hierarchical BH mergers, and other relevant astrophysical processes. A key distinction between the analytic estimates of Sec. III and the N-body/semianalytical simulations presented here is that the latter self-consistently evolve the cluster over time [73,75,103]. As binaries harden in the cluster core, energy conservation requires that the liberated binding energy be deposited into the surrounding stellar population. This drives cluster expansion via Hénon's principle [104] and causes the half-mass radius to grow secularly [80,105,106]. Simultaneously, BH ejections through dynamical recoil reduce the total cluster mass. Together, these two effects cause the cluster escape velocity, $v_{esc} \propto \sqrt{M_{cl}/r_h}$, to decrease monotonically over time.

A. Postprocessing existing cluster simulations

We begin by postprocessing existing *indirect* N-body and semianalytical star cluster simulations spanning a grid of initial cluster properties, including the number of stars, half-mass radius, and metallicity. These simulations are routinely used to understand the binary properties of GW sources and to compare with detected events. They therefore provide an ideal and well-tested framework for our investigation. Here, we use only publicly available cluster evolution data from the CMC [77][4] and COLOSSUS [107][5] catalogs. These frameworks model stellar evolution, relaxation-driven structural changes, and the dynamical interactions that lead to BH mergers. Here, we only mention the physics included in the simulation without elaborating the details of their implementation.

Each cluster simulation starts with N stars drawn from a chosen Kroupa initial mass function at a chosen metallicity, with a half-mass radius of r_h. This translates to an initial total cluster mass. The evolution framework then maps the ZAMS mass distribution to compact remnants using precomputed stellar-evolution prescriptions and computes the initial cluster mass, velocity dispersion, and escape velocity under the assumption of virial equilibrium. The cluster subsequently evolves through stellar-evolution mass loss, two-body relaxation, and evaporation, all of which reduce $M_{cl}(t)$ and $v_{esc}(t)$ while driving an expansion of $r_h(t)$. The time dependence of the escape velocity is particularly important for determining whether BH merger remnants remain bound to the cluster.

Within this evolving background, BH binaries form and merge through multiple dynamical channels, including three-body binary formation, binary-single, and binary-binary encounters and GW captures in close passages. These frameworks further employ mass-weighted pairing, which preferentially selects the most massive BHs when forming binaries and therefore facilitates hierarchical growth when remnants are retained. Both for two-body and three-body dynamical interactions, the BH masses are chosen using a mass-weighted distribution. For more details, we refer the readers to Refs. [75,77].

For each BH merger event, the code computes the remnant mass, spin, and GW recoil kick. For the kick, the default choice is to use HLZ prescription. A remnant is retained if its recoil velocity is smaller than v_{esc} at the time

[4]https://cmc.ciera.northwestern.edu/BBHmergers_CMCcatalog.dat.
[5]https://cmc.ciera.northwestern.edu/BBHmergers_colossus.dat.

of merger; otherwise, it is ejected and removed from further evolution. This setup enables us to track the formation pathways and hierarchical assembly of BHs within a self-consistently evolving cluster environment.

Another important piece of physics included in these simulations is the effect of binary-single interactions. Exchange encounters preferentially replace the lighter BH in a binary with a more massive incoming BH, thereby increasing the binary mass and tending to produce mass ratios closer to unity. Repeated dynamical encounters also harden the binary by decreasing its semmajor axis. These processes play a key role in shaping the masses, mass ratios, and merger timescales of dynamically formed BBHs in dense star clusters.

The CMC cluster simulations span a $4 \times 4 \times 3 \times 3$ grid in the following parameters: the number of particles $N = \{2 \times 10^5, 4 \times 10^5, 8 \times 10^5, 1.6 \times 10^6\}$, the initial virial radius $r_\mathrm{v} = \{0.5, 1, 2, 4\}$ pc, the metallicity $Z/Z_\odot = \{0.01, 0.1, 1\}$, and the galactocentric distance $R_\mathrm{gc} = \{2, 8, 20\}$ kpc. These parameters are chosen to broadly represent globular clusters in the Milky Way. Here, N denotes the initial number of stars, r_v is the virial radius which is related to the half-mass radius through $r_\mathrm{h} = 0.8 r_\mathrm{v}$, and R_gc is the galactocentric distance. On the other hand, the COLOSSUS cluster simulations assume an initial virial radius $r_v = 2$ pc, an initial metallicity $Z = 0.1 Z_\odot$, and a galactocentric radius $R_\mathrm{gc} = 20$ kpc in a Milky Way–like environment, with the number of particles set to $N = 10^7$. This implies that the virial escape velocities of clusters [computed using Eq. (6)] in the CMC simulations lie in the range 15.9–127.0 $\mathrm{km\,s^{-1}}$, while the corresponding escape velocities in the COLOSSUS simulations extend up to 158.8 $\mathrm{km\,s^{-1}}$. These values characterize the clusters on the scale of their half-mass radii; the central escape velocities are expected to be substantially larger.

We first postprocess the BBH mergers from the CMC catalog. In the leftmost panel of Fig. 10, we compare the mass-ratio distribution of all mergers with that of the $1\mathrm{G} + 1\mathrm{G}$ mergers. We find a large abundance of nearly equal-mass BBHs. Naturally, we find a large peak at $q \sim 1$ in the $1\mathrm{G} + 1\mathrm{G}$ case. All 1G BHs are assumed to be nonspinning in the CMC catalog. Using this population, we compute the recoil kick velocities for all $1\mathrm{G} + 1\mathrm{G}$ mergers with the gwModel_flow_prec and HLZ prescriptions, finding that both models predict very similar kick velocities. Consequently, they yield comparable mass and spin distributions for the retained 2G BHs.

Because the underlying mass and spin distributions of 1G and 2G BHs are nearly identical for both recoil prescriptions, we consistently postprocess the subsequent $2\mathrm{G} + 1\mathrm{G}$ mergers using both models. We focus on $2\mathrm{G} + 1\mathrm{G}$, as it produces the largest number of mergers after the $1\mathrm{G} + 1\mathrm{G}$ mergers. The mass-ratio distribution for $2\mathrm{G} + 1\mathrm{G}$ mergers peaks around $q \sim 2$. In this regime, the gwModel_flow_prec and HLZ prescriptions predict noticeably different recoil kick velocities, leading to distinct mass and spin distributions for the retained 3G BHs. For reference, we also show the inferred masses and spins of the two BHs involved in GW231123.

Next, we shift our focus to the COLOSSUS catalog. As before, we find no significant differences in the recoil kick velocities for $1\mathrm{G} + 1\mathrm{G}$ mergers, nor in the resulting mass and spin distributions of the retained 2G BHs. However, the recoil kick velocities for $2\mathrm{G} + 1\mathrm{G}$ mergers differ noticeably between the gwModel_flow_prec and HLZ prescriptions. As a result, these differences lead to slightly different mass and spin distributions for the retained 3G BHs.

B. New semianalytical cluster simulations with RAPSTER

Motivated by the results above, we perform new semi-analytical cluster simulations using RAPSTER. We adopt RAPSTER over the CMC code primarily for computational efficiency: RAPSTER simulates a full globular cluster evolution on a single CPU in under a minute, orders of magnitude faster than Monte Carlo *indirect* N-body codes. This speedup arises because RAPSTER foregoes individual particle tracking entirely, instead evolving a small set of global cluster properties (core density, velocity dispersion, and BH population) and treating each dynamical channel (three-body binary formation, exchange encounters, and GW captures) as a Poisson process with analytically prescribed rates. This makes RAPSTER well suited for population-level studies requiring large number of cluster simulations. One other difference between RAPSTER and CMC is that RAPSTER explicitly tracks mergers from long-lived dynamically assembled triples undergoing Lidov-Kozai oscillations as a distinct formation channel, whereas CMC only encounters such configurations transiently during few-body scattering integrations. For a detailed description of the code and its underlying prescriptions, we refer the reader to Ref. [85].

We simulate BH mergers in three representative clusters with different cluster mass M_cl and half-mass radius r_h (and therefore different initial escape velocities) using RAPSTER. Rather than simulating a large ensemble of clusters with different initial conditions, we choose to simulate three representative clusters using 2500 independent random seeds. This allows us to isolate the impact of different recoil-kick prescriptions on the astrophysical interpretation of hierarchical BH mergers. The representative clusters were chosen such that their final mass and radius is close to the median of the Galactic Globular Cluster Database[6] (version 4) [108].[7]

[6] https://people.smp.uq.edu. au/HolgerBaumgardt/globular/parameter.html.

[7] For the Baumgardt catalog, we find a median cluster mass of $M_\mathrm{cl} = 1.15^{+2.29}_{-0.84} \times 10^5 M_\odot$ and a median projected half-light radius of $r_{h,l} = 3.18^{+3.92}_{-1.16}$ pc, where the uncertainties denote the 16th and 84th percentiles.

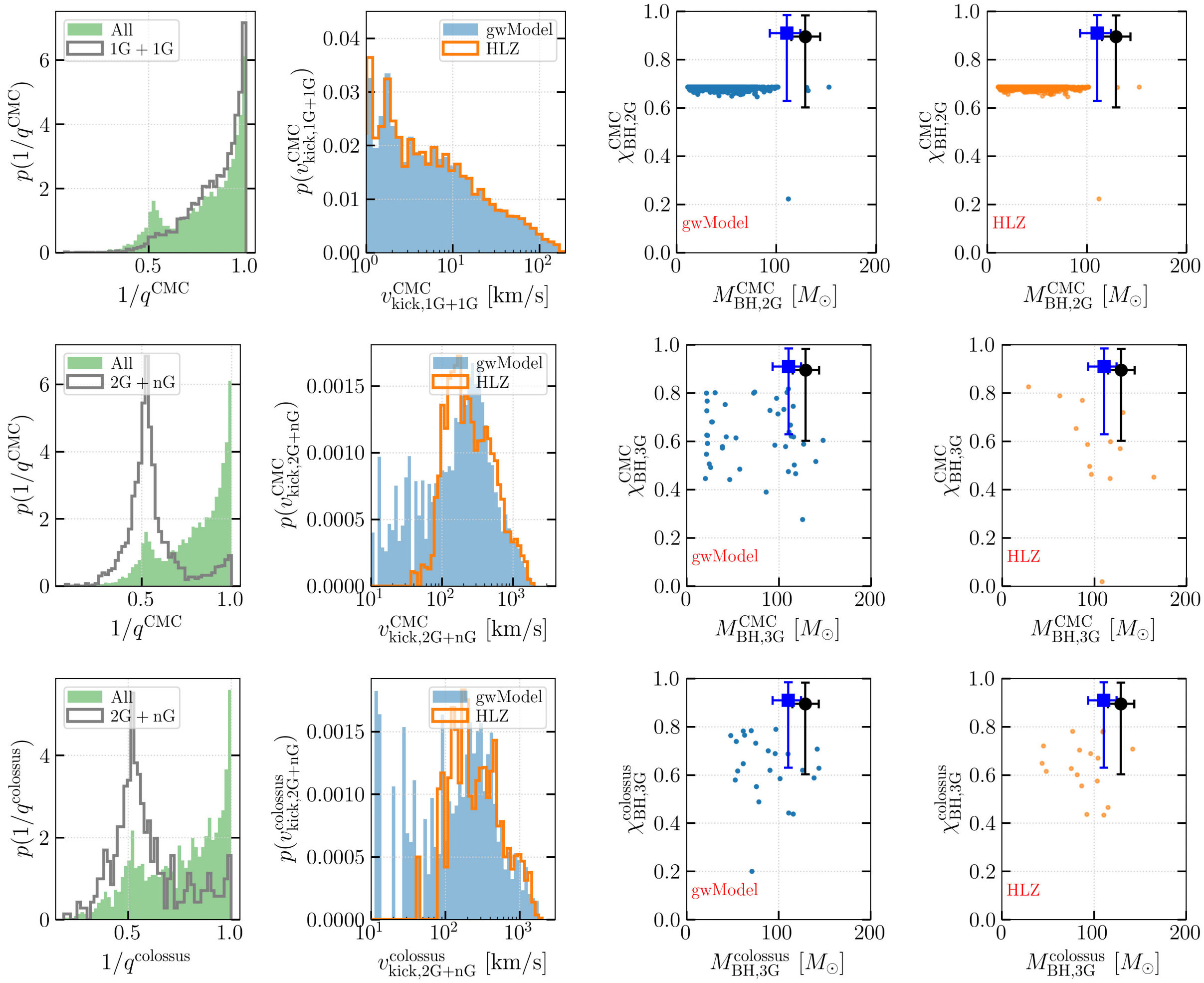

FIG. 10. We now test the two recoil-kick models using detailed cluster-evolution simulations (CMC and COLOSSUS) that self-consistently model the cluster evolution and BH mergers. Upper panels: he leftmost panel shows the mass-ratio distribution of all mergers (green) and $1\mathrm{G}+1\mathrm{G}$ mergers only (gray), obtained from the CMC catalog. The second panel shows the recoil kick velocities for all $1\mathrm{G}+1\mathrm{G}$mergers. The third and fourth panels show the mass and spin distributions of the *retained remnant BHs* after $1\mathrm{G}+1\mathrm{G}$ mergers. We find that, because 1G BHs are nonspinning, both recoil prescriptions yield similar kick velocities and produce similar mass and spin distributions for the retained 2G BHs. We show analogous results for $2\mathrm{G}+1\mathrm{G}$ mergers of the CMC catalog (center panels), where the mass ratios are more asymmetric and the BH spins are nonzero. The differences between the gwModel_flow_prec and HLZ recoil velocities are less pronounced compared to previous Figs. 6 and 7, but they are still noteworthy. The models also yield slightly different mass and spin distributions for the retained 3G BHs. Finally, we show the analogous results for $2\mathrm{G}+1\mathrm{G}$ mergers from the COLOSSUS (bottom panels) catalog. For reference, we also show the inferred mass and spin of the two BHs involved in GW231123 (as black and blue markers with error-bars). Details are in Sec. IV A.

The first representative cluster has $N=2.5\times10^{6}$ stars drawn at metallicity $Z=0.002$ (roughly 10% of the solar metallicity), and with a half-mass radius of $r_{\rm h}=1$ pc. This corresponds to an initial total cluster mass of $\sim1.5\times10^{6}M_\odot$ since the initial average stellar mass is $\simeq0.6M_\odot$. We also adopt slightly different assumptions for the initial BH populations and binary interactions compared to the previous subsection. Such modifications are straightforward to implement in semianalytical frameworks like RAPSTER as it enables thousands of simulations to be performed within a relatively short time. We simulate clusters in which the initial BH masses are drawn uniformly from $[3,60]M_\odot$, while the BH spins are drawn uniformly from [0, 1]. We adopt random mass pairing in both two-body and three-body interactions. All other aspects of the binary hardening prescription are kept unchanged from the default implementation in RAPSTER. We adopt these choices in order to maintain consistency with the default setup of the back-of-the-envelope calculations presented in Secs. III A and III C.

For this cluster, we find an initial escape velocity of $v^{0}_{\rm esc}\sim100\ \mathrm{km\,s^{-1}}$. We first examine the mass-ratio and recoil kick velocity distributions of all mergers (Fig. 11). For the $1\mathrm{G}+1\mathrm{G}$ population, we find that the kick

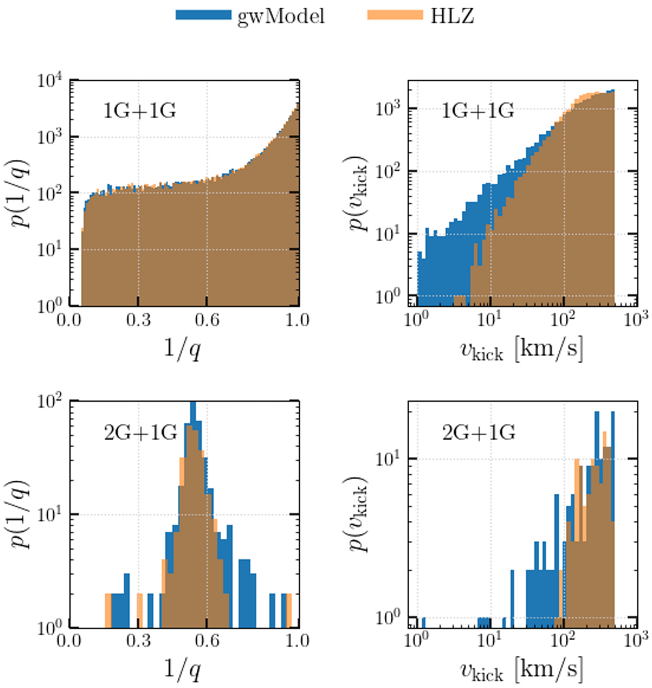

FIG. 11. Similar to the left two columns of Fig. 10 but for semianalytical code RAPSTER. Here, we do not show results for an ensemble of clusters but instead for a representative cluster with different random seeds for sampling the BH masses and spins magnitude and direction. The cluster is initiated with $N = 2.5 \times 10^6$ stars drawn at metallicity $Z = 0.002$, and with a half-mass radius of $r_h = 1$ pc (i.e., with initial escape velocity of ~ 100 km s^{-1}). Details are in Sec. IV B.

distributions predicted by the two models differ noticeably: gwModel_flow_prec yields a larger fraction of low-velocity kicks compared to HLZ. We find that 40,616 mergers occur in-cluster when gwModel_flow_prec is used, compared to 40,765 when HLZ is employed. For gwModel_flow_prec (HLZ), approximately 6% (3%) of 1G + 1G mergers produce recoil velocities below 50 km s^{-1}. These fractions increase to 13% (9%), 27% (26%), and 57% (57%) for recoil thresholds of 100, 150, and 500 km s^{-1}, respectively. Overall, 7% (3.7%) of all mergers yield recoil velocities below the initial escape velocity of $v^0_{\rm esc} \sim 100$ km s^{-1} when using gwModel_flow_prec (HLZ). This means that they retain different number of BHs in the next generation. For 2G + 1G mergers, these differences within the escape velocity become more pronounced. For higher-generation mergers, the number of mergers is comparatively small, but we still observe a systematic trend in which gwModel_flow_prec predicts smaller recoil velocities than HLZ. For example, we record 372 in-cluster 2G + 1G mergers when using gwModel_flow_prec, whereas HLZ yields 241 such mergers. We find that gwModel_flow_prec predicts that approximately 4% of these mergers have recoil velocities below 50 km s^{-1}, while HLZ yields none in this range. This behavior is consistent with the increasing divergence between the models at larger mass ratios, where HLZ exhibits more extended high-velocity tails. To quantify these differences, we compute the JSD between the distributions predicted by gwModel_flow_prec and HLZ. For the 1G + 1G population, the mass-ratio distributions are nearly identical, with JSD = 0.0004, while the kick-velocity distributions differ more substantially, yielding JSD = 0.1741. For the 2G + 1G population, the differences become significantly larger: the mass-ratio distributions have JSD = 0.0525, whereas the kick-velocity distributions have JSD = 0.5854. These results quantitatively confirm that the largest discrepancies between the recoil prescriptions arise for mergers involving higher-generation BHs, where differences in the predicted kick velocities strongly affect remnant retention and subsequent hierarchical growth.

In Fig. 12 (first column), we show the mass and spin distributions of retained BHs across different merger generations using two recoil-kick prescriptions: gwModel_flow_prec and HLZ. The distributions of retained 2G and 3G BHs differ substantially. We find that none of the models predict a population of retained 4G BHs. For the retained 2G BH population, we obtain JSD = 0.029 for the mass distribution and JSD = 0.0164 for the spin distribution. These relatively small values indicate that the shapes of the retained 2G mass and spin distributions are broadly similar under the two recoil prescriptions. However, the total numbers of retained BHs differ substantially between the models. We emphasize that the JSD is computed using normalized distributions and therefore quantifies differences in distribution shape rather than differences in the absolute number of retained BHs.

Next, we simulate a slightly less massive cluster, initialized with $N = 10^6$ stars at metallicity $Z = 0.002$ and with a half-mass radius of $r_h = 1$ pc. This corresponds to an initial total cluster mass of $\sim 5.9 \times 10^5 M_\odot$ and an initial escape velocity of $v^0_{\rm esc} \sim 63$ km s^{-1}. We adopt the same initial mass and spin distributions for the BHs as in the previous case. As before, we find significant differences in the properties of retained 2G BHs between the two recoil prescriptions. In particular, gwModel_flow_prec retains 533 2G BHs, compared to only 173 for HLZ. The corresponding JSDs are JSD = 0.1062 for the mass distribution and JSD = 0.0532 for the spin distribution. These values are noticeably larger than those obtained for the previous cluster, indicating that the retained 2G populations differ not only in number but also in the shapes of their mass and spin distributions. In addition, we find that none of the 2 G + n G merger remnants are retained in this cluster.

Finally, we simulate a light cluster, initialized with $N = 3.4 \times 10^5$ stars at metallicity $Z = 0.002$ and with a half-mass radius of $r_h = 4$ pc (Fig. 12, third column). This corresponds to an initial total cluster mass of $\sim 2 \times 10^5 M_\odot$ and an initial escape velocity of $v^0_{\rm esc} \sim 18$ km s^{-1}. We find that none of the 2G BHs are retained when the HLZ model

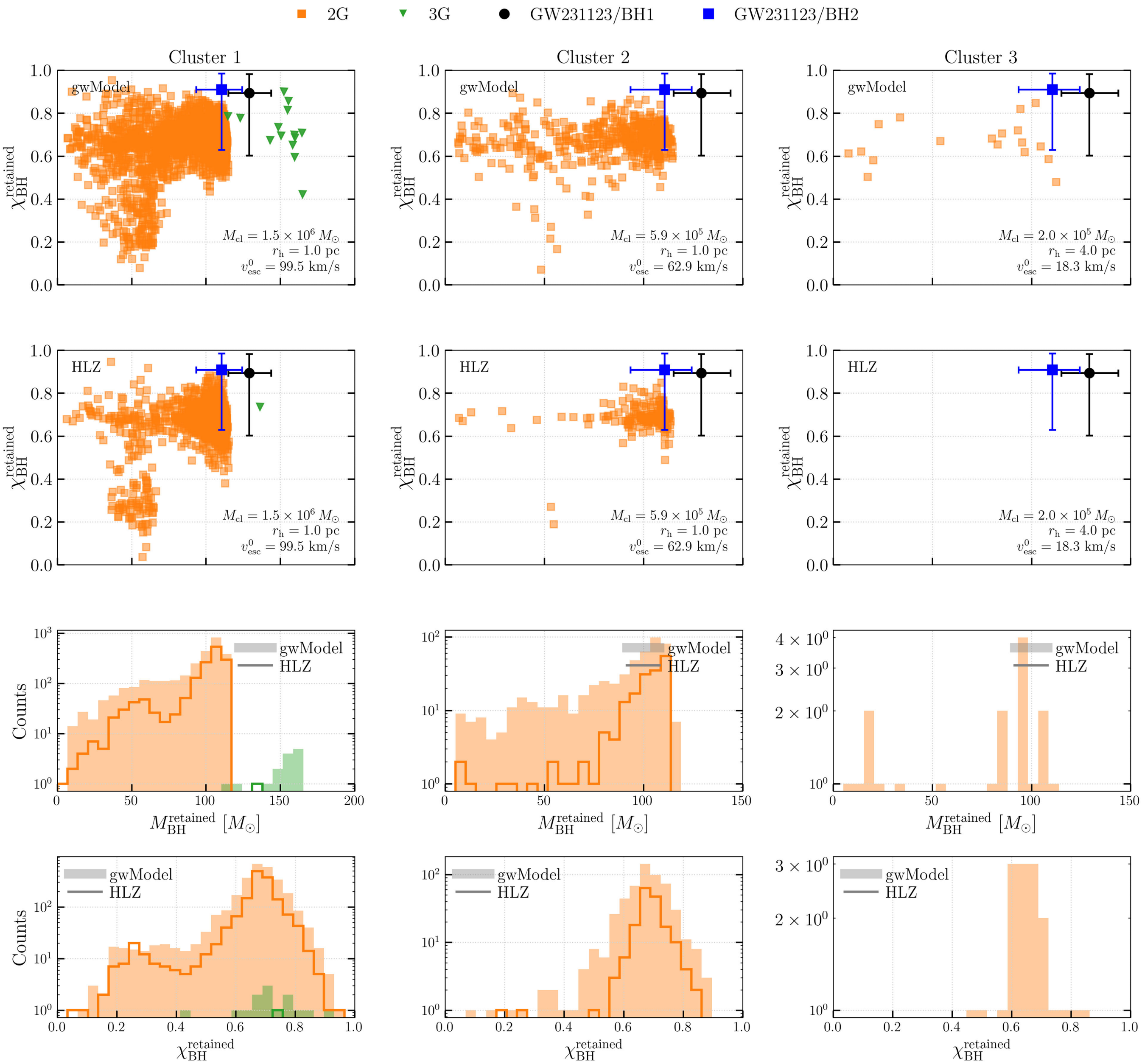

FIG. 12. Similar to Fig. 11 but showing the mass and spin distributions of retained BHs in different RAPSTER simulations from the two recoil kick models. We show results from three distinct clusters (each with 2500 realizations). The clusters have initial escape velocities of ∼99.5, ∼62.9, and ∼18.3 $\mathrm{km\,s^{-1}}$, respectively, and were chosen such that their final mass and radius ($M_{cl} \sim 2 \times 10^5 M_\odot$ and $R_{cl} \sim 4$ pc) is close to the median of the Galactic Globular Cluster Database,[5] Version 4 [108]. The lowest panel shows the 1D histogram of the retained remnant masses. For reference, we again show the inferred mass and spin of the two BHs involved in GW231123. Details are in Sec. IV B.

is used. In contrast, gwModel_flow_prec yields a small population (18) of retained 2G BHs. As before, no 2 G + n G merger remnants are retained.

These results provide useful demonstrations of the impact of recoil kicks on hierarchical BBH mergers in clusters and motivate a comprehensive exploration across a wide range of cluster initial conditions, initial BH populations, and binary interaction prescriptions. Such an extended study is beyond the scope of the present analysis and will be pursued in a follow-up investigation.

V. CONCLUSIONS

In this paper, we performed a detailed study of hierarchical BH mergers in clusters using a newly developed and more accurate recoil-kick model for BBH mergers, gwModel_flow_prec [48], and compared its results with the widely-used analytic model HLZ [9,22,23,29,30].

We used a variety of theoretical astrophysical toy models of star clusters to understand the recoil-kick model systematics and to address several astrophysically interesting questions, such as the following. How massive can BHs become purely through hierarchical mergers? How do the BH mass and spin distributions evolve across successive generations? How frequently are BH merger remnants retained within a cluster? How do the initial mass and spin distributions of 1G BHs and their binary pairing functions affect hierarchical-merger outcomes? These simplified toy models allow us to isolate and understand the impact of recoil-kick modeling choices without additional astrophysical complications. We then used a detailed semianalytical framework for cluster evolution (RAPSTER) and also used previous simulation catalogs to investigate how more complex physical processes, such as cluster expansion, evaporation, binary hardening, and dynamical exchanges, modify hierarchical-merger pathways and their observable consequences.

We showed that, in most cases, the updated gwModel_flow_prec prescription leads to the formation of more massive BHs through hierarchical mergers compared to the HLZ model that has been employed in essentially all N-body and population-synthesis frameworks to date. Furthermore, gwModel_flow_prec produces a significantly larger number of BHs that occupy the binary-parameter space corresponding to the progenitor BHs inferred for GW231123, whereas HLZ struggles to populate this region in most cases.

As a byproduct of our analysis, we confirm previous findings that the initial BH population, the binary pairing function, and the prescription for binary hardening have significant impacts on hierarchical-merger outcomes. This underscores the importance of performing multiple simulations that systematically vary these physical ingredients as well as the recoil kick prescriptions in order to fully capture the range of possible hierarchical-merger pathways.

Since our study highlights the importance of using accurate recoil-kick prescriptions in cluster-evolution modeling, it is natural to incorporate such prescriptions into other semianalytical cluster-evolution frameworks, such as FASTCLUSTER [79], cBHBd [80], B-POP [81], and SEVN [61], as well as into direct N-body and Monte Carlo cluster codes, including Cluster Monte Carlo [75,77], MOCCA [109], NBODY6++GPU [103], and PETAR [110]. This is an avenue we will pursue in more details in future work. Recently, Ref. [111] performed semianalytical cluster simulations using NR- and BHPT-based surrogate recoil models. We expect that increasingly accurate recoil prescriptions will be adopted in future studies of hierarchical mergers and cluster evolution. We will also explore distilling our normalizing flow model for $v_{\rm kick}$ into a closed-form conditional distribution via symbolic regression. A compact analytic expression would be straightforward to incorporate into existing cluster simulation codes without external ML package dependencies (e.g., PYTORCH and NFLOWS), while also reducing the per-sample computational cost relative to neural network inference.

Another important avenue for future work is to perform cluster-evolution simulations across a broader range of cluster properties using gwModel_flow_prec in order to determine how hierarchical-merger pathways change relative to those predicted by HLZ. It will be particularly interesting to assess whether this leads to a significantly larger population of massive BHs in clusters and thereby provides a more natural explanation for events such as GW231123. We will leave this investigation to future work.

ACKNOWLEDGMENTS

We thank Emanuele Berti, Katie Breivik, Maya Fishbach, Norbert Langer, Carl Rodriguez, and Tejaswi Venumadhav for discussion. T. I. is supported in part by the National Science Foundation under Grant No. NSF PHY-2309135 and the Gordon and Betty Moore Foundation Grant No. GBMF7392. Use was made of computational facilities purchased with funds from the National Science Foundation (CNS-1725797) and administered by the Center for Scientific Computing (CSC). The C. S. C. is supported by the California NanoSystems Institute and the Materials Research Science and Engineering Center (MRSEC; NSF DMR 2308708) at University of California Santa Barbara. D. W. and K. K. are supported by NSF Grants No. AST-2307146, No. PHY-2513337, No. PHY-090003, and No. PHY-20043; by NASA Grant No. 21-ATP21-0010; by John Templeton Foundation Grant No. 62840; by the Simons Foundation [Grant No. MPS-SIP-00001698 (E. B.)]; by the Simons Foundation International (Grant No. SFI-MPS-BH-00012593-02); and by Italian Ministry of Foreign Affairs and International Cooperation Grant No. PGR01167. In addition, K. K. is supported by the Onassis Foundation Scholarship No. F ZT 041-1/2023-2024. This work was carried out at the Advanced Research Computing at Hopkins (ARCH) core facility ([112]), which is supported by the NSF Grant No. OAC-1920103.

DATA AVAILABILITY

There are no publicly available research data or software supporting this manuscript. Requests for further information or data should be sent to the authors.

[1] John G. Baker, Joan Centrella, Dae-Il Choi, Michael Koppitz, James R. van Meter, and M. Coleman Miller, Getting a kick out of numerical relativity, Astrophys. J. Lett. **653**, L93 (2006).

[2] Manuela Campanelli, Carlos O. Lousto, Yosef Zlochower, and David Merritt, Maximum gravitational recoil, Phys. Rev. Lett. **98**, 231102 (2007).

[3] Hiroyuki Nakano, Manuela Campanelli, Carlos O. Lousto, and Yosef Zlochower, Perturbative effects of spinning black holes with applications to recoil velocities, Classical Quantum Gravity **28**, 134005 (2011).

[4] Bernd Bruegmann, Jose A. Gonzalez, Mark Hannam, Sascha Husa, and Ulrich Sperhake, Exploring black hole superkicks, Phys. Rev. D **77**, 124047 (2008).

[5] Manuela Campanelli, Carlos O. Lousto, Yosef Zlochower, and David Merritt, Large merger recoils and spin flips from generic black-hole binaries, Astrophys. J. Lett. **659**, L5 (2007).

[6] Dae-Il Choi, Bernard J. Kelly, William D. Boggs, John G. Baker, Joan Centrella, and James van Meter, Recoiling from a kick in the head-on collision of spinning black holes, Phys. Rev. D **76**, 104026 (2007).

[7] Sergio Dain, Carlos O. Lousto, and Yosef Zlochower, Extra-Large remnant recoil velocities and spins from near-extremal-bowen-york-spin black-hole binaries, Phys. Rev. D **78**, 024039 (2008).

[8] Jose A. Gonzalez, Ulrich Sperhake, Bernd Bruegmann, Mark Hannam, and Sascha Husa, Total recoil: The maximum kick from nonspinning black-hole binary inspiral, Phys. Rev. Lett. **98**, 091101 (2007).

[9] J. A. Gonzalez, M. D. Hannam, U. Sperhake, Bernd Bruegmann, and S. Husa, Supermassive recoil velocities for binary black-hole mergers with antialigned spins, Phys. Rev. Lett. **98**, 231101 (2007).

[10] James Healy, Frank Herrmann, Ian Hinder, Deirdre M. Shoemaker, Pablo Laguna, and Richard A. Matzner, Superkicks in hyperbolic encounters of binary black holes, Phys. Rev. Lett. **102**, 041101 (2009).

[11] James Healy and Carlos O. Lousto, Ultimate black hole recoil: What is the maximum high-energy collision kick?, Phys. Rev. Lett. **131**, 071401 (2023).

[12] John G. Baker, William D. Boggs, Joan Centrella, Bernard J. Kelly, Sean T. McWilliams, M. Coleman Miller, and James R. van Meter, Modeling kicks from the merger of non-precessing black-hole binaries, Astrophys. J. **668**, 1140 (2007).

[13] John G. Baker, William D. Boggs, Joan Centrella, Bernard J. Kelly, Sean T. McWilliams, M. Coleman Miller, and James R. van Meter, Modeling kicks from the merger of generic black-hole binaries, Astrophys. J. Lett. **682**, L29 (2008).

[14] F. Herrmann, I. Hinder, D. Shoemaker, and P. Laguna, Binary black holes and recoil velocities, AIP Conf. Proc. **873**, 89 (2006).

[15] Carlos O. Lousto and Yosef Zlochower, Further insight into gravitational recoil, Phys. Rev. D **77**, 044028 (2008).

[16] Frank Herrmann, Ian Hinder, Deirdre Shoemaker, Pablo Laguna, and Richard A. Matzner, Gravitational recoil from spinning binary black hole mergers, Astrophys. J. **661**, 430 (2007).

[17] Frank Herrmann, Ian Hinder, Deirdre M. Shoemaker, Pablo Laguna, and Richard A. Matzner, Binary black holes: Spin dynamics and gravitational recoil, Phys. Rev. D **76**, 084032 (2007).

[18] Frank Herrmann, Ian Hinder, Deirdre Shoemaker, and Pablo Laguna, Unequal mass binary black hole plunges and gravitational recoil, Classical Quantum Gravity **24**, S33 (2007).

[19] Kelly Holley-Bockelmann, Kayhan Gultekin, Deirdre Shoemaker, and Nico Yunes, Gravitational wave recoil and the retention of intermediate mass black holes, Astrophys. J. **686**, 829 (2008).

[20] Jose Luis Jaramillo, Rodrigo Panosso Macedo, Philipp Moesta, and Luciano Rezzolla, Black-hole horizons as probes of black-hole dynamics I: Post-merger recoil in head-on collisions, Phys. Rev. D **85**, 084030 (2012).

[21] Michael Koppitz, Denis Pollney, Christian Reisswig, Luciano Rezzolla, Jonathan Thornburg, Peter Diener, and Erik Schnetter, Recoil velocities from equal-mass binary-black-hole mergers, Phys. Rev. Lett. **99**, 041102 (2007).

[22] Carlos O. Lousto and Yosef Zlochower, Modeling gravitational recoil from precessing highly-spinning unequal-mass black-hole binaries, Phys. Rev. D **79**, 064018 (2009).

[23] Carlos O. Lousto and Yosef Zlochower, Modeling maximum astrophysical gravitational recoil velocities, Phys. Rev. D **83**, 024003 (2011).

[24] Jeremy D. Schnittman, Alessandra Buonanno, James R. van Meter, John G. Baker, William D. Boggs, Joan Centrella, Bernard J. Kelly, and Sean T. McWilliams, Anatomy of the binary black hole recoil: A multipolar analysis, Phys. Rev. D **77**, 044031 (2008).

[25] Carlos F. Sopuerta, Nicolas Yunes, and Pablo Laguna, Gravitational recoil velocities from eccentric binary black hole mergers, Astrophys. J. Lett. **656**, L9 (2007).

[26] Denis Pollney *et al.*, Recoil velocities from equal-mass binary black-hole mergers: A systematic investigation of spin-orbit aligned configurations, Phys. Rev. D **76**, 124002 (2007).

[27] Luciano Rezzolla, Rodrigo P. Macedo, and Jose Luis Jaramillo, Understanding the "anti-kick" in the merger of binary black holes, Phys. Rev. Lett. **104**, 221101 (2010).

[28] Carlos O. Lousto and Yosef Zlochower, Hangup kicks: Still larger recoils by partial spin/orbit alignment of black-hole binaries, Phys. Rev. Lett. **107**, 231102 (2011).

[29] Carlos O. Lousto and Yosef Zlochower, Nonlinear gravitational recoil from the mergers of precessing black-hole binaries, Phys. Rev. D **87**, 084027 (2013).

[30] Carlos O. Lousto, Yosef Zlochower, Massimo Dotti, and Marta Volonteri, Gravitational recoil from accretion-aligned black-hole binaries, Phys. Rev. D **85**, 084015 (2012).

[31] Sarah H. Miller and R. A. Matzner, Multipole analysis of kicks in collision of binary black holes, Gen. Relativ. Gravit. **41**, 525 (2009).

[32] Wolfgang Tichy and Pedro Marronetti, Binary black hole mergers: Large kicks for generic spin orientations, Phys. Rev. D **76**, 061502 (2007).

[33] Yosef Zlochower, Manuela Campanelli, and Carlos O. Lousto, Modeling gravitational recoil using numerical relativity, Classical Quantum Gravity **28**, 114015 (2011).

[34] James Healy, Carlos O. Lousto, and Yosef Zlochower, Remnant mass, spin, and recoil from spin aligned black-hole binaries, Phys. Rev. D **90**, 104004 (2014).

[35] Carlos O. Lousto, Manuela Campanelli, Yosef Zlochower, and Hiroyuki Nakano, Remnant masses, spins and recoils from the merger of generic black-hole binaries, Classical Quantum Gravity **27**, 114006 (2010).

[36] Pranesh A. Sundararajan, Gaurav Khanna, and Scott A. Hughes, Binary black hole merger gravitational waves and recoil in the large mass ratio limit, Phys. Rev. D **81**, 104009 (2010).

[37] Tousif Islam, Scott E. Field, and Gaurav Khanna, Remnant black hole properties from numerical-relativity-informed perturbation theory and implications for waveform modeling, Phys. Rev. D **108**, 064048 (2023).

[38] Scott A. Hughes, Marc Favata, and Daniel E. Holz, How black holes get their kicks: Radiation recoil in binary black hole mergers, in *Growing Black Holes: Accretion in a Cosmological Context* (Springer, Berlin, Heidelberg, 2004).

[39] Richard H. Price, Gaurav Khanna, and Scott A. Hughes, Black hole binary inspiral and trajectory dominance, Phys. Rev. D **88**, 104004 (2013).

[40] Richard H. Price, Gaurav Khanna, and Scott A. Hughes, Systematics of black hole binary inspiral kicks and the slowness approximation, Phys. Rev. D **83**, 124002 (2011).

[41] Luc Blanchet, Moh’d S. S. Qusailah, and Clifford M. Will, Gravitational recoil of inspiralling black-hole binaries to second post-Newtonian order, Astrophys. J. **635**, 508 (2005).

[42] Carlos F. Sopuerta, Nicolas Yunes, and Pablo Laguna, Gravitational recoil from binary black hole mergers: The close-limit approximation, Phys. Rev. D **74**, 124010 (2006); **75**, 069903(E) (2007); **78**, 049901(E) (2008).

[43] Marc Favata, Scott A. Hughes, and Daniel E. Holz, How black holes get their kicks: Gravitational radiation recoil revisited, Astrophys. J. Lett. **607**, L5 (2004).

[44] M. J. Fitchett, The influence of gravitational wave momentum losses on the centre of mass motion of a Newtonian binary system, Mon. Not. R. Astron. Soc. **203**, 1049 (1983).

[45] M. J. Fitchett and Steven L. Detweiler, Linear momentum and gravitational-waves—circular orbits around a Schwarzschild black-hole, Mon. Not. R. Astron. Soc. **211**, 933 (1984).

[46] Alan G. Wiseman, Coalescing binary systems of compact objects to (post)5/2 Newtonian order. 2. Higher order wave forms and radiation recoil, Phys. Rev. D **46**, 1517 (1992).

[47] Lawrence E. Kidder, Coalescing binary systems of compact objects to postNewtonian 5/2 order. 5. Spin effects, Phys. Rev. D **52**, 821 (1995).

[48] Tousif Islam and Digvijay Wadekar, Accurate models for recoil velocity distribution in black hole mergers with comparable to extreme mass-ratios and their astrophysical implications, Phys. Rev. D **113**, 104017 (2026).

[49] Yosef Zlochower and Carlos O. Lousto, Modeling the remnant mass, spin, and recoil from unequal-mass, precessing black-hole binaries: The intermediate mass ratio regime, Phys. Rev. D **92**, 024022 (2015); **94**, 029901(E) (2016).

[50] James R. van Meter, M. Coleman Miller, John G. Baker, William D. Boggs, and Bernard J. Kelly, A general formula for black hole gravitational wave kicks, Astrophys. J. **719**, 1427 (2010).

[51] Vijay Varma, Scott E. Field, Mark A. Scheel, Jonathan Blackman, Davide Gerosa, Leo C. Stein, Lawrence E. Kidder, and Harald P. Pfeiffer, Surrogate models for precessing binary black hole simulations with unequal masses, Phys. Rev. Res. **1**, 033015 (2019).

[52] Vijay Varma, Davide Gerosa, Leo C. Stein, François Hébert, and Hao Zhang, High-accuracy mass, spin, and recoil predictions of generic black-hole merger remnants, Phys. Rev. Lett. **122**, 011101 (2019).

[53] David Merritt, Milos Milosavljevic, Marc Favata, Scott A. Hughes, and Daniel E. Holz, Consequences of gravitational radiation recoil, Astrophys. J. Lett. **607**, L9 (2004).

[54] U. Sperhake, R. Rosca-Mead, D. Gerosa, and E. Berti, Amplification of superkicks in black-hole binaries through orbital eccentricity, Phys. Rev. D **101**, 024044 (2020).

[55] Parthapratim Mahapatra, Anuradha Gupta, Marc Favata, K. G. Arun, and B. S. Sathyaprakash, Remnant black hole kicks and implications for hierarchical mergers, Astrophys. J. Lett. **918**, L31 (2021).

[56] Vijay Varma, Sylvia Biscoveanu, Tousif Islam, Feroz H. Shaik, Carl-Johan Haster, Maximiliano Isi, Will M. Farr, Scott E. Field, and Salvatore Vitale, Evidence of large recoil velocity from a black hole merger signal, Phys. Rev. Lett. **128**, 191102 (2022).

[57] Tousif Islam, Avi Vajpeyi, Feroz H. Shaik, Carl-Johan Haster, Vijay Varma, Scott E. Field, Jacob Lange, Richard O’Shaughnessy, and Rory Smith, Analysis of GWTC-3 with fully precessing numerical relativity surrogate models, Phys. Rev. D **112**, 044001 (2025).

[58] Juan Calderón Bustillo, Samson H. W. Leong, and Koustav Chandra, GW190412: Measuring a black-hole recoil direction through higher-order gravitational-wave modes, Nat. Astron. **9**, 1530 (2025).

[59] Davide Gerosa and Christopher J. Moore, Black hole kicks as new gravitational wave observables, Phys. Rev. Lett. **117**, 011101 (2016).

[60] Angela Borchers, Claire S. Ye, and Maya Fishbach, Gravitational-wave kicks impact the spins of black holes from hierarchical mergers, Astrophys. J. **987**, 146 (2025).

[61] Mario Spera and Michela Mapelli, Very massive stars, pair-instability supernovae and intermediate-mass black holes with the SEVN code, Mon. Not. R. Astron. Soc. **470**, 4739 (2017).

[62] Gabriele Franciolini, Konstantinos Kritos, Luca Reali, Floor Broekgaarden, and Emanuele Berti, Observing black hole mergers beyond the pair-instability mass gap with next-generation gravitational wave detectors, Phys. Rev. D **110**, 023036 (2024).

[63] Emanuele Berti, Michael Kesden, and Ulrich Sperhake, Effects of post-Newtonian spin alignment on the distribution of black-hole recoils, Phys. Rev. D **85**, 124049 (2012).

[64] Kayhan Gultekin, M. Coleman Miller, and Douglas P. Hamilton, Growth of intermediate—mass black holes in globular clusters, Astrophys. J. **616**, 221 (2004).

[65] Davide Gerosa, Nicola Giacobbo, and Alberto Vecchio, High mass but low spin: An exclusion region to rule out hierarchical black-hole mergers as a mechanism to populate the pair-instability mass gap, Astrophys. J. **915**, 56 (2021).

[66] Davide Gerosa and Emanuele Berti, Are merging black holes born from stellar collapse or previous mergers?, Phys. Rev. D **95**, 124046 (2017).

[67] Vishal Baibhav, Davide Gerosa, Emanuele Berti, Kaze W. K. Wong, Thomas Helfer, and Matthew Mould, The mass gap, the spin gap, and the origin of merging binary black holes, Phys. Rev. D **102**, 043002 (2020).

[68] Yann Bouffanais, Michela Mapelli, Davide Gerosa, Ugo N. Di Carlo, Nicola Giacobbo, Emanuele Berti, and Vishal Baibhav, Constraining the fraction of binary black holes formed in isolation and young star clusters with gravitational-wave data, Astrophys. J. **886**, 25 (2019).

[69] R. Abbott *et al.* (LIGO Scientific and Virgo Collaborations), GW190521: A binary black hole merger with a total mass of $150 M_{\odot}$, Phys. Rev. Lett. **125**, 101102 (2020).

[70] A. G. Abac *et al.* (LIGO Scientific, Virgo, and KAGRA Collaborations), GW231123: A binary black hole merger with total mass 190–265 MSun, Astrophys. J. Lett. **993**, L25 (2025).

[71] Michael Zevin and Daniel E. Holz, Avoiding a cluster catastrophe: Retention efficiency and the binary black hole mass spectrum, Astrophys. J. Lett. **935**, L20 (2022).

[72] Stefano Torniamenti, Michela Mapelli, Carole Périgois, Manuel Arca Sedda, Maria Celeste Artale, Marco Dall'Amico, and Maria Paola Vaccaro, Hierarchical binary black hole mergers in globular clusters: Mass function and evolution with redshift, Astron. Astrophys. **688**, A148 (2024).

[73] Manuel Arca Sedda, Albrecht W. H. Kamlah, Rainer Spurzem, Francesco Paolo Rizzuto, Thorsten Naab, Mirek Giersz, and Peter Berczik, The dragon-II simulations—II. Formation mechanisms, mass, and spin of intermediate-mass black holes in star clusters with up to 1 million stars, Mon. Not. R. Astron. Soc. **526**, 429 (2023).

[74] Sambaran Banerjee, Stellar-mass black holes in young massive and open stellar clusters—IV. Updated stellar-evolutionary and black hole spin models and comparisons with the LIGO-Virgo O1/O2 merger-event data, Mon. Not. R. Astron. Soc. **500**, 3002 (2020).

[75] Carl L. Rodriguez, Michael Zevin, Pau Amaro-Seoane, Sourav Chatterjee, Kyle Kremer, Frederic A. Rasio, and Claire S. Ye, Black holes: The next generation—repeated mergers in dense star clusters and their gravitational-wave properties, Phys. Rev. D **100**, 043027 (2019).

[76] Konstantinos Kritos, Emanuele Berti, and Joseph Silk, Massive black hole assembly in nuclear star clusters, Phys. Rev. D **108**, 083012 (2023).

[77] Kyle Kremer, Claire S. Ye, Nicholas Z. Rui, Newlin C. Weatherford, Sourav Chatterjee, Giacomo Fragione, Carl L. Rodriguez, Mario Spera, and Frederic A. Rasio, Modeling dense star clusters in the Milky Way and beyond with the CMC cluster catalog, Astrophys. J. Suppl. Ser. **247**, 48 (2020).

[78] Barry McKernan, K. E. Saavik Ford, Harrison E. Cook, Vera Delfavero, Emily McPike, Kaila Nathaniel, Jake Postiglione, Shawn Ray, and Richard O'Shaughnessy, McFACTS I: Testing the LVK AGN channel with Monte Carlo for AGN channel testing and simulation (McFACTS), Astrophys. J. **990**, 217 (2025).

[79] Michela Mapelli, Yann Bouffanais, Filippo Santoliquido, Manuel Arca Sedda, and M. Celeste Artale, The cosmic evolution of binary black holes in young, globular, and nuclear star clusters: Rates, masses, spins, and mixing fractions, Mon. Not. R. Astron. Soc. **511**, 5797 (2022).

[80] Fabio Antonini and Mark Gieles, Population synthesis of black hole binary mergers from star clusters, Mon. Not. R. Astron. Soc. **492**, 2936 (2020).

[81] Manuel Arca Sedda, Michela Mapelli, Matthew Benacquista, and Mario Spera, Isolated and dynamical black hole mergers with B-POP: The role of star formation and dynamics, star cluster evolution, natal kicks, mass and spins, and hierarchical mergers, Mon. Not. R. Astron. Soc. **520**, 5259 (2023).

[82] Francesco Paolo Rizzuto, Thorsten Naab, Antti Rantala, Peter H. Johansson, Jeremiah P. Ostriker, Nicholas C. Stone, Shihong Liao, and Dimitrios Irodotou, The growth of intermediate mass black holes through tidal captures and tidal disruption events, Mon. Not. R. Astron. Soc. **521**, 2930 (2023).

[83] Konstantinos Kritos, Luca Reali, Ken K. Y. Ng, Fabio Antonini, and Emanuele Berti, Gravitational wave inference of star cluster properties from intermediate-mass black hole mergers, Phys. Rev. D **111**, 063056 (2025).

[84] Lavinia Paiella, Manuel Arca Sedda, Benedetta Mestichelli, and Cristiano Ugolini, Seeds to success: Growing heavy black holes in dense star clusters, Astron. Astrophys. **708**, A200 (2026).

[85] Konstantinos Kritos, Vladimir Strokov, Vishal Baibhav, and Emanuele Berti, Dynamical formation of black hole binaries in dense star clusters: Rapid cluster evolution code, Phys. Rev. D **110**, 043023 (2024).

[86] José Tomas Galvez Ghersi and Leo C Stein, A fixed point for black hole distributions, Classical Quantum Gravity **38**, 045012 (2021).

[87] J. Lin, Divergence measures based on the shannon entropy, IEEE Trans. Inf. Theory **37**, 145 (1991).

[88] Davide Gerosa and Emanuele Berti, Escape speed of stellar clusters from multiple-generation black-hole mergers in the upper mass gap, Phys. Rev. D **100**, 041301 (2019).

[89] Giacomo Fragione, Abraham Loeb, and Frederic A. Rasio, On the origin of GW190521-like events from repeated black hole mergers in star clusters, Astrophys. J. Lett. **902**, L26 (2020).

[90] K. Belczynski *et al.*, The effect of pair-instability mass loss on black hole mergers, Astron. Astrophys. **594**, A97 (2016).

[91] R. Farmer, M. Renzo, S. E. de Mink, P. Marchant, and S. Justham, Mind the gap: The location of the lower edge of the pair instability supernovae black hole mass gap, Astrophys. J. **88**, 53 (2019).

[92] Jim Fuller and Linhao Ma, Most black holes are born very slowly rotating, Astrophys. J. Lett. **881**, L1 (2019).

[93] R. Abbott *et al.* (KAGRA, Virgo, and LIGO Scientific Collaborations), Population of merging compact binaries inferred using gravitational waves through GWTC-3, Phys. Rev. X **13**, 011048 (2023).

[94] Jarrod R. Hurley, Onno R. Pols, and Christopher A. Tout, Comprehensive analytic formulae for stellar evolution as a function of mass and metallicity, Mon. Not. R. Astron. Soc. **315**, 543 (2000).

[95] Jarrod R. Hurley, Christopher A. Tout, and Onno R. Pols, Evolution of binary stars and the effect of tides on binary populations, Mon. Not. R. Astron. Soc. **329**, 897 (2002).

[96] Sambaran Banerjee, Krzysztof Belczynski, Christopher L. Fryer, Peter Berczik, Jarrod R. Hurley, Rainer Spurzem, and Long Wang, BSE versus StarTrack: Implementations of new wind, remnant-formation, and natal-kick schemes in NBODY7 and their astrophysical consequences, Astron. Astrophys. **639**, A41 (2020).

[97] S. E. Woosley and Alexander Heger, The pair-instability mass gap for black holes, Astrophys. J. Lett. **912**, L31 (2021).

[98] Simon F. Portegies Zwart, Holger Baumgardt, Piet Hut, Junichiro Makino, and Stephen L. W. McMillan, Formation of massive black holes through runaway collisions in dense young star clusters, Nature (London) **428**, 724 (2004).

[99] Kyle Kremer, Mario Spera, Devin Becker, Sourav Chatterjee, Ugo N. Di Carlo, Giacomo Fragione, Carl L. Rodriguez, Claire S. Ye, and Frederic A. Rasio, Populating the upper black hole mass gap through stellar collisions in young star clusters, Astrophys. J. **903**, 45 (2020).

[100] M. Atakan Gürkan, John M. Fregeau, and Frederic A. Rasio, Massive black hole binaries from collisional runaways, Astrophys. J. Lett. **640**, L39 (2006).

[101] Enrico Barausse, Viktoriya Morozova, and Luciano Rezzolla, On the mass radiated by coalescing black-hole binaries, Astrophys. J. **758**, 63 (2012); **786**, 76(E) (2014).

[102] Enrico Barausse and Luciano Rezzolla, Predicting the direction of the final spin from the coalescence of two black holes, Astrophys. J. Lett. **704**, L40 (2009).

[103] Long Wang, Rainer Spurzem, Sverre Aarseth, Keigo Nitadori, Peter Berczik, M. B. N. Kouwenhoven, and Thorsten Naab, NBODY6++GPU: ready for the gravitational million-body problem, Mon. Not. R. Astron. Soc. **450**, 4070 (2015).

[104] M. H. Hénon, The Monte Carlo method, Astrophys. Space Sci. **14**, 151 (1971).

[105] Oleg Y. Gnedin, Jeremiah P. Ostriker, and Scott Tremaine, Co-evolution of galactic nuclei and globular cluster systems, Astrophys. J. **785**, 71 (2014).

[106] M. Gieles and H. Baumgardt, Lifetimes of tidally limited star clusters with different radii, Mon. Not. R. Astron. Soc. **389**, L28 (2008).

[107] Aidan Mai, Kyle Kremer, and Fulya Kiroglu, Shadows of the colossus: Hierarchical black hole mergers in a 10-million-body globular cluster simulation, Astrophys. J. **998**, 138 (2026).

[108] H. Baumgardt and M. Hilker, A catalogue of masses, structural parameters, and velocity dispersion profiles of 112 Milky Way globular clusters, Mon. Not. R. Astron. Soc. **478**, 1520 (2018).

[109] Mirek Giersz, Douglas C. Heggie, Jarrod R. Hurley, and Arkadiusz Hypki, MOCCA code for star cluster simulations —II. Comparison with N-body simulations, Mon. Not. R. Astron. Soc. **431**, 2184 (2013).

[110] Long Wang, Masaki Iwasawa, Keigo Nitadori, and Junichiro Makino, PETAR: A high-performance N-body code for modelling massive collisional stellar systems, Mon. Not. R. Astron. Soc. **497**, 536 (2020).

[111] Debatri Chattopadhyay, Daniel Marín Pina, Mark Gieles, Fabio Antonini, and Fotios Fronimos Pouliasis, Repopulating the pair-instability mass gap without sustained growth to massive IMBHs: The case of 47 Tuc, arXiv:2604.09773.

[112] https://www.arch.jhu.edu/.